The contribution of residential coal combustion to atmospheric PM$_{2.5}$ in the North China during winter

Pengfei Liu[1, 3], **Chenglong Zhang**[1, 2, 3], **Chaoyang Xue**[1, 3], **Yujing Mu**[1, 2, 3, 4], **Junfeng Liu**[1, 2, 3], **Yuanyuan Zhang**[1, 2, 3], **Di Tian**[1, 3], **Can Ye**[1, 3], **Hongxing Zhang**[1, 5], **Jian Guan**[6]

[1] Research Center for Eco-Environmental Sciences, Chinese Academy of Sciences, Beijing, 100085, China

[2] Center for Excellence in Urban Atmospheric Environment, Institute of Urban Environment, Chinese Academy of Sciences, Xiamen, 361021, China

[3] University of Chinese Academy of Sciences, Beijing, 100049, China

[4] National Engineering Laboratory for VOCs Pollution Control Material & Technology, University of Chinese Academy of Sciences, Beijing, 100049, China

[5] Beijing Urban Ecosystem Research Station, Beijing, 100085, China

[6] Environment Monitoring Station of Baoding City, Hebei, 071000, China

Correspondence to: Yujing Mu (yjmu@rcees.ac.cn)

Abstract: The vast area in the North China, especially during wintertime, is currently suffering from severe haze events due to the high levels of atmospheric PM$_{2.5}$. To recognize the reasons for the high levels of PM$_{2.5}$, daily samples of PM$_{2.5}$ were simultaneously collected at the four sampling sites of Beijing City (BJ), Baoding City (BD), Wangdu County (WD) and Dongbaituo Countryside (DBT) during the winters and springs of 2014-2015. The concentrations of the typical water-soluble ions (WSIs, such as Cl$^-$, NO$_3^-$, SO$_4^{2-}$ and NH$_4^+$) at DBT were found to be remarkably higher than those at BJ in the two winters, but almost the same as those at BJ in the two springs. The evidently greater concentrations of OC, EC and secondary inorganic ions (NO$_3^-$, SO$_4^{2-}$, NH$_4^+$ and Cl$^-$) at DBT than at WD, BD and BJ during the winter of 2015 indicated that the pollutants in the rural area were not due to transportation from its neighbor cities but dominated by local emissions. As the distinct source for atmospheric OC and EC in the rural area, the residential coal combustion also made contribution to secondary inorganic ions through the emissions of their precursors (NO$_x$, SO$_2$, NH$_3$ and HCl) as well as heterogeneous or multiphase reactions on the surface of OC and EC. The average mass proportions of OC, EC, NO$_3^-$ and SO$_4^{2-}$ at BD and WD were found to be very close to those at DBT, but evidently different from those at BJ, implying that the pollutants in the cities of WD and BD which are fully surrounded by the countryside were strongly affected by the residential coal combustion. The OC/EC ratios at the four sampling sites became the almost same value of 4.8 when the concentrations of PM$_{2.5}$ were greater than 150 μg m^{-3}, suggesting that the residential coal combustion could also make dominant contribution to atmospheric PM$_{2.5}$ at BJ during the severe pollution period when the air parcels were usually from southwest–south regions where high density of farmers reside. The evident increase of the number of the species involved in significant correlations from the countryside to the cities further confirmed that residential coal combustion was preferentially dominant source for the key species in the rural area whereas the complex sources including local emissions and regional transportation were dominant for atmospheric species in the cities. The significant correlations among OC, EC, Cl$^-$, NO$_3^-$, and NH$_4^+$ were found at the four sampling sites but only significant correlation between OC (or EC) and SO$_4^{2-}$ was found at BJ, implying that the formation rate of

41 SO_4^{2-} via heterogeneous or multiphase reactions might be relatively slower than those of NO_3^-,

42 NH_4^+ and Cl^-. Based on the chemical mass closure (CMC) method, the contributions of the

43 primary particle emission from residential coal combustion to atmospheric $PM_{2.5}$ at BJ, BD, WD

44 and DBT were estimated to be 32 %, 49 %, 43 % and 58 %, respectively.

45 **1 Introduction**

46 In recent years, the vast area in the North China is frequently suffering from severe haze pollution

47 (Chan and Yao, 2008; Zhang et al., 2012; Zhang et al., 2015), which has aroused great attention to

48 the public (Guo et al., 2014; Huang et al., 2014; Cheng et al., 2016; Wang et al., 2016; J. Liu et al.,

49 2016). The severe haze pollution is mainly due to the high level of fine particulate matters with

50 dynamic diameter less than 2.5μm ($PM_{2.5}$) (Huang et al., 2014; P. Liu et al., 2016). $PM_{2.5}$ can

51 reduce atmospheric visibility by absorbing or scattering the incident light (Buseck and Posfai,

52 1999; Cheng et al., 2006) and increase morbidity and mortality by penetrating the human bronchi

53 and lungs (Nel, 2005; Poschl, 2005; Peplow, 2014).

54 To alleviate the serious haze pollution problems, the Chinese government has performed a series

55 of control measures for major pollution sources (Zhang et al., 2012; J. Liu et al., 2016; Li et al.,

56 2016b; Wen et al., 2016). For example, coal-fired power plants have been forced to install flue gas

57 desulfurization and denitration (Zhang et al., 2012; Chen et al., 2014), coal has been replaced with

58 natural gas and electricity in megacities (Wang et al., 2009; Duan et al., 2012; Zhao et al., 2013a;

59 Tan et al., 2016), stricter emission standards have been implemented for vehicles and industrial

60 boilers (Zhang et al., 2012; Tang et al., 2016) and so on, resulting in the decrease trend of primary

61 pollutants including $PM_{2.5}$ in recent years (Ma et al., 2016; Wen et al., 2016; Zhang et al., 2016).

62 However, the $PM_{2.5}$ levels still achieved to be above 1000 μg m^{-3} in some areas of

63 Beijing-Tianjin-Hebei (BTH) region during the period of the red alert for haze in December 2016

64 (http://english.mep.gov.cn/News_service/media_news/201612/t20161220_369317.shtml)   when

65   the stricter control measures (e.g. stop production for industries and construction, and the odd and

66   even number rule) had been performed (Y. Li et al., 2016), implying that sources other than

67   industries, construction and vehicles might make dominant contribution to atmospheric $PM_{2.5}$ in

68   the region. Residential coal combustion which is prevailing for heating during winter in the region

69   was suspected to be a dominant source for atmospheric $PM_{2.5}$. Although annual residential coal

70   consumption (about 4,200,000 kg) in BTH region only accounts for small fraction (about 11 %) of

71   the total coal consumption (http://www.qstheory.cn/st/dfst/201306/t20130607_238302.htm), the

72   emission factors of primary pollutants including $PM_{2.5}$ from the residential coal combustion have

73   been found to be about 1-3 orders of magnitude greater than those from coal combustion of

74   industries and power plants (Revuelta et al., 1999; Chen et al., 2005; Xu et al., 2006; Zhang et al.,

75   2008; Geng et al., 2014; Yang et al., 2016). In addition, annual residential coal consumption

76   mainly focuses on the four months in winter. Although the Chinese government has implemented

77   control measures for residential coal combustion (e.g. replacement of traditional coal stoves by

78   new stoves, bituminous coal by anthracite, and coal by electricity and natural gas), the promotion

79   strength of the control measures is still very limited. Additionally, the promotion new stoves are

80   still with strong smoke emission due to lack of clean combustion technique, and the anthracite is

81   not welcomed by farmers because of its extremely slow combustion rate in comparison with

82   bituminous coal.

83   There were few studies focusing on the influence of residential coal combustion on atmospheric

84   particles in the North China. W. Li et al. (2014) concluded that strong sources for PM_{10} in rural

85   residential areas were from household solid fuel combustion, based on annual mean PM_{10}

86   concentrations observed in urban regions (180 ± 171 μg m^{-3}) and rural villages (182 ± 154 μg m^{-3})

87 in the northern China. Duan et al. (2012) inferred that the lower OC/EC ratios at the rural site than

88 at the urban site were ascribed to coal combustion prevailed in the rural area. Our previous study

89 revealed that residential coal combustion made evident contribution to atmospheric water-soluble

90 ions (WSIs) in Beijing (P. Liu et al., 2016). Based on Weather Research and Forecasting model

91 coupled with Chemistry, J. Liu et al. (2016) recently estimated that the residential sources (solid

92 fuel) contributed 32 % and 53 % of the primary $PM_{2.5}$ emissions in the BTH region during the

93 whole year and during the winter of 2010, respectively.

94 In this study, daily samples of $PM_{2.5}$ were simultaneously collected at the four sampling sites

95 (Beijing City, Baoding City, Wangdu County and Dongbaituo Countryside) during the winters and

96 springs of 2014-2015, and the direct evidence for the influence of residential coal combustion on

97 regional $PM_{2.5}$ in the region was found based on the $PM_{2.5}$ levels, the $PM_{2.5}$ composition

98 characteristics, the correlations among the key species in $PM_{2.5}$, the back trajectories and the

99 chemical mass closure method.

100 **2 Materials and methods**

101 **2.1 Sampling sites**

102 The two sampling sites in Beijing City and Dongbaituo Countryside, which have been described

103 in detail by our previous study (P. Liu et al., 2016), were selected on a rooftop (approximately 25

104 m and 5 m above ground, respectively) of the Research Center for Eco-Environmental Sciences,

105 Chinese Academy of Sciences (RCEES, CAS) and a field station in the agricultural field of

106 Dongbaituo village, Baoding, Hebei Province, respectively. Another two sampling sites in

107 Baoding City and Wangdu County were both chosen on the rooftop of local environmental

108 monitor station (about 30 m and 20 m above ground, respectively), which are both located in the

109   center of the cities and surrounded by some commercial and residential areas. The spatial locations

110   of the four sampling sites are presented in Fig. 1 and the distances between Beijing and Baoding,

111   Baoding and Wangdu, Wangdu and Dongbaituo are about 156 km, 36 km and 12 km, respectively.

112   Thereafter, the sampling sites of Beijing, Baoding, Wangdu and Dongbaituo are abbreviated as BJ,

113   BD, WD and DBT, respectively.

114   **2.2 Sample collection and analysis**

115   $PM_{2.5}$ samples at BJ and DBT were collected simultaneously on PTFE filters (90 mm, Millipore)

116   by medium-volume $PM_{2.5}$ samplers (LaoYing-2034) at a flow rate of 100 L min^{-1} from January 15,

117   2014 to May 31, 2015, in winter (January 15, 2014-Febrary 25, 2014, November 18, 2014-January

118   20, 2015 and February 11, 2015-March 15, 2015) and spring (April 21, 2014-May 4, 2014 and

119   March 20, 2015-May 31, 2015). An enhanced observation at BJ, BD, WD and DBT was carried

120   out from January 21 to February 10, 2015 and $PM_{2.5}$ samples were collected in the same way on

121   the quartz fiber filters (90 mm, Munktell). The sampling duration was 24 h (from 15:00 p.m. to

122   15:00 p.m. of the following day in local time (UTC + 8)). All the samples were put in the

123   appropriative dishes (90 mm, Millipore) after sampling and preserved in a refrigerator

124   immediately until analysis.

125   As for the quartz fiber filters, half of each filter was extracted ultrasonically with 10 mL ultrapure

126   water for half an hour. The solutions were filtered through a micro-porous membrane (pore size,

127   0.45 μm; diameter, 13 mm) before analysis and the WSIs (Cl^-, NO_3^-, SO_4^{2-}, Na^+, NH_4^+, Mg^{2+}, Ca^{2+}

128   and K^+) in the treated filtrates were analyzed by Ion Chromatography (IC, WAYEE IC6200) which

129   has been described in detail by our previous study (P. Liu et al., 2016). A quarter of each filter was

130   cut into fragments and digested with 5 mL 65 % HNO_3 and 2 mL 30 % H_2O_2 (Li et al., 2015) by a

5

131   microwave digestion system (SINEO, MASTER-40). The digestion solution was diluted to 25 mL

132   with ultrapure water to insure the solution acidity below 10 % and the trace elements (Al, Mn, Fe,

133   Cu, Zn, As, Se, Sr, Tl and Pb) in the diluted solution were analyzed by a triple-quadrupole

134   inductively coupled plasma mass spectrometry (ICP-MS/MS, Agilent 8800). The standard

135   reference material (GBW07427) was also digested as the same way as the samples and the

136   recoveries of the trace elements were within the allowable ranges of the certified values (100 $\pm$

137   15 %). Another quarter of each filter was analyzed by a DRI thermal optical carbon analyzer

138   (DRI-2001A) for carbon components (OC and EC). In addition, the PTFE filters were only used

139   for analyzing the WSIs (P. Liu et al., 2016).

140   **2.3 Chemical mass closure**

141   Chemical mass closure (CMC) method was adopted by considering secondary inorganic aerosols

142   (SIA, the sum of SO_4^{2-}, NO_3^- and NH_4^+), sea salt & coal combustion (derived from Cl^- and Na^+),

143   biomass burning (characterized by K^+), mineral dust, EC, primary organic carbon (POC),

144   secondary organic carbon (SOC) and trace element oxide (TEO) (Hsu et al., 2010b; Zhang et al.,

145   2013; Mantas et al., 2014; Tian et al., 2014; Kong et al., 2015).

146   Atmospheric Na^+ and Cl^- were considered to be from sea salt (Brewer, 1975; van Eyk et al., 2011),

147   coal combustion (Bläsing and Müller, 2012; Yu et al., 2013; Wu et al., 2014; He et al., 2015; P. Liu

148   et al., 2016) and biomass burning (Zong et al., 2016; Yao et al., 2016). However, biomass burning

149   in the NCP region is mainly focusing on the harvest seasons in summer and autumn (Zong et al.,

150   2016), and few farmers are currently combusting crop straws for household cooking and heating

151   because of the inconvenience of biomass with respect to coal and liquid gas. Thus, only sea salt

152   and coal combustion were considered for the estimation of mass concentrations for atmospheric

153   Na^+ and Cl^- in this study based on the following equations:

154     $[Cl_{cc}^-] + [Cl_{ss}^-] = [Cl^-]$ (1)

155     $[Na_{cc}^+] + [Na_{ss}^+] = [Na^+]$ (2)

156     $\dfrac{[Cl_{cc}^-]/35.5}{[Na_{cc}^+]/23} = 1.4$ (3)

157     $\dfrac{[Cl_{ss}^-]/35.5}{[Na_{ss}^+]/23} = 1.18$ (4)

158   where [Cl⁻ss] and [Na⁺ss] are the mass concentrations of Cl⁻ and Na⁺ from sea salt, and [Cl⁻cc] and

159   [Na⁺cc] are the mass concentrations of Cl⁻ and Na⁺ from coal combustion. The molar ratio of Cl⁻ss

160   to Na⁺ss was adopted to be 1.18 which represented the typical ratio from sea salt (Brewer, 1975).

161   The molar ratio of Cl⁻cc to Na⁺cc was chosen to be 1.4 in this study according to our preliminary

162   measurements from the raw bituminous coal prevailed in the North China and the value of 1.4 has

163   been recorded by the previous study (Bläsing and Müller, 2012). If the molar ratios of atmospheric

164   Cl⁻ to Na⁺ in $PM_{2.5}$ were greater than the value of 1.4 or lower than the value of 1.18, atmospheric

165   Cl⁻ and Na⁺ would be considered to be totally from coal combustion or sea salt.

166   Because the average Al content accounts for about 7 % in mineral dust (Zhang et al., 2003; Ho et

167   al., 2006; Hsu et al., 2010a; Zhang et al., 2013), the mineral dust was estimated based on the

168   follow equation:

169     $[Mineral\ dust] = \dfrac{[Al]}{0.07}$ (5)

170   POC and SOC were calculated by the EC-tracer OC/EC method (Cheng et al., 2011; Zhao et al.,

171   2013b; G. J. Zheng et al., 2015; Cui et al., 2015) as follows:

172     $[POC] = [EC] \times (\frac{[OC]}{[EC]})_{pri} = K[EC] + M$ (6)

173     $[SOC] = [OC] - [POC]$ (7)

174   The values of K and M are estimated by linear regression analysis using the data pairs with the

175   lowest 10 % percentile of ambient OC/EC ratios. It should be mentioned that POC could be

176   underestimated and SOC could be overestimated by the EC-tracer OC/EC method, because the

177   lowest 10 % percentile of OC/EC ratios measured were usually less than those from dominant

178   sources of coal combustion and biomass burning in autumn and winter (Ding et al., 2012; Cui et

179   al., 2015).

180   To estimate the contribution of heavy metal oxide, the enrichment factors (EF) of various heavy

181   metal elements were calculated by the following equation (Hsu et al., 2010b; Zhang et al., 2013):

182    $$\mathrm{EF} = \frac{(^{[Element]}\!/_{[Al]})_{aerosol}}{(^{[Element]}\!/_{[Al]})_{crust}} \tag{8}$$

183   where ([Element]/[Al])$_{aerosol}$ is the ratio of the element to Al in aerosols and ([Element]/[Al])$_{crust}$ is

184   the ratio of the element to Al in the average crust (Taylor, 1964). According to the method

185   developed by Landis et al. (2001), the atmospheric concentrations of elements were multiplied by

186   a factor of 0, 0.5 and 1 if their EFs were less than 1, between 1 and 5, and greater than 5,

187   respectively. Based on the EFs (Fig. 2), the equation for estimating TEO was derived as following:

188    $$[TEO] = 1.3 \times ([Cu] + [Zn] + [Pb] + [As] + [Se] + [Tl] + 0.5 \times [Mn]) \tag{9}$$

189   The value of 1.3 was the conversion factor of metal abundance to oxide abundance. It should be

190   mentioned that some other elements such as Cd and Ba were not measured in this study, probably

191   resulting in underestimating the proportion of TEO. Nevertheless, the biases are probably

192   insignificant because the proportion of TEO only accounted for less than 2 % in PM$_{2.5}$.

193   **2.4 Meteorological, trace gases and back trajectory**

194   Both the meteorological data, including wind speed, wind direction, relative humidity (RH),

195   temperature, barometric pressure and air quality index (AQI) of PM$_{2.5}$, SO$_2$, NO$_2$, CO, O$_3$ at BJ,

BD and WD were obtained from Beijing urban ecosystem research station in RCEES, CAS

(http://www.bjurban.rcees.cas.cn/), environmental protection bureau of Baoding City

(http://bdhb.gov.cn/) and environmental monitoring station of Wangdu County

(http://www.wdx.gov.cn/), respectively. The meteorological data at BJ and BD are shown in Fig. 3

and the average concentrations of SO_2 and NO_2 at BJ, BD and WD are listed in Table 2 during the

sampling period in the winter of 2015, which will be discussed in section 3.2 and 3.3.

The air mass backward trajectories were calculated for 24 h through the National Oceanic and

Atmospheric Administration (NOAA) Hybrid Single-Particle Lagrangian Integrated Trajectory

Version 4 model (HYSPLIT 4 model) with National Centers for Environmental Prediction's

(NCEP) global data. The backward trajectories arriving at 500 m above sampling position were

computed at 0:00 h, 6:00 h, 12:00 h and 18:00 h (UTC) for each sampling day, respectively. A

K-means cluster method was then used for classifying the trajectories into several different

clusters and suitable clusters were selected for further analysis.

3 Results and discussion

3.1 Comparison of atmospheric WSIs between the two sampling sites of BJ and DBT

The daily variations of atmospheric WSIs during the sampling periods at BJ and DBT are shown

in Fig. 4. It is evident that the variations of the WSIs between the two sampling sites of BJ and

DBT exhibited similar trend, but the mass concentrations of the WSIs were remarkably greater at

DBT than at BJ during the two winter seasons. As listed in Table 1, the average concentrations of

the typical WSIs were a factor of 1.5-2.0 greater at DBT than at BJ during the two winter seasons,

whereas they were approximately the same at the two sampling sites during the two spring seasons.

To clearly reveal the differences, the daily D-values (the concentrations of WSIs at DBT minus

218   those at BJ) of several typical WSIs as well as the total WSIs between the two sampling sites of

219   DBT and BJ are individually illustrated in Fig. 5. With only the exception for Ca^{2+} (typical

220   mineral dust component), the D-values of NH_4^+, NO_3^-, SO_4^{2-} and Cl^- between the two sampling

221   sites of DBT and BJ exhibited obviously positive values during the most sampling days in the two

222   winter seasons, implying that the sources related to mineral dust could be excluded for explaining

223   the obviously higher concentrations of the WSIs at DBT than at BJ. The sampling site of DBT is

224   adjacent to Baoding city where the AQI during the winter always ranked the top three among

225   Chinese cities in recent years (http://113.108.142.147:20035/emcpublish/), and hence the

226   relatively greater concentrations of the WSIs at DBT might be due to the regional pollution.

227   However, the emissions of pollutants from industries, power plants and vehicles are usually

228   relatively stable, which could not account for the remarkable differences of the D-values between

229   the winters and the springs (Fig. 5). If the relatively high concentrations of the WSIs at DBT

230   during the winter were ascribed to the regional pollution, there would be additional strong sources

231   for them in the area of Baoding. To explore whether the regional pollution was responsible for the

232   relatively high concentrations of the WSIs at DBT in winter, the various species in $PM_{2.5}$ collected

233   simultaneously at DBT and its neighbor cities of WD, BD and BJ in the winter of 2015 were

234   further investigated in the following section.

235   **3.2 Daily variations of the species in $PM_{2.5}$ at the four sampling sites**

236   The daily variations of the species in $PM_{2.5}$ at the four sampling sites also exhibited similar

237   fluctuation trends (Fig. 6), but there was obvious difference (p < 0.01) in the concentrations of OC,

238   EC, NH_4^+, NO_3^-, SO_4^{2-}, Cl^- and K^+ among the four sampling sites, ranked in order as BJ < WD <

239   BD < DBT. The meteorological conditions, especially wind speed and planetary boundary layer

240   (PBL), play pivotal roles in the dispersion and accumulation of atmospheric pollutants (Xu et al.,

241   2011; Tao et al., 2012; Sun et al., 2013; Chen et al., 2015; Gao et al., 2016), which can cause

242   spatial and temporal difference of pollutants. As for the sampling sites of BD, WD and DBT, the

243   meteorological conditions could be considered as the same because of the short distances (< 36

244   km) among them, and hence the spatial difference of $PM_{2.5}$ and the major components at the three

245   sampling sites was rationally ascribed to the different source strengths. Although the distance

246   between the sampling sites of BJ and BD is about 156 km, there was no significant difference of

247   the wind speeds between the two sampling sites during the sampling period (1.4 ± 1.4 m/s for BJ

248   and 1.7 ± 1.1 m/s for BD, Fig. 3). Therefore, the spatial difference of $PM_{2.5}$ and the major

249   components between the sampling sites of BJ and the other three could not be ascribed to the

250   difference of the wind speeds. Because the information of PBL was not available in the region of

251   Baoding, it is difficult to discuss the impact of PBL on the spatial difference of the pollutants. As

252   listed in Table 2, the average concentration of the total species at DBT was about a factor of 2.7,

253   1.8 and 1.4 higher than those at BJ, WD and BD, respectively. The largest levels of the key species

254   in $PM_{2.5}$ at DBT among the four sampling sites implied that the pollutants at the rural site were not

255   through the air parcel transportation from its neighbor cities but mainly ascribed to the local

256   emissions or formation. Vehicles and industries could be rationally excluded for explaining the

257   largest levels of the key species in $PM_{2.5}$ at DBT, because these sources are very sparse in the rural

258   area around DBT (See section 3.4). Compared with the cities, the distinct source for atmospheric

259   pollutants at DBT in winter is the residential coal combustion which is prevailingly used for

260   heating and cooking in rural areas of the Northern China. The emissions of various pollutants from

261   residential coal combustion were very serious due to lack of any control measures, strong smoke

11

262   could be seen in the chimney of the residential coal stoves. The emission factors of OC and EC

263   from residential coal combustion were reported to be 0.47-7.82 g kg^{-1} coal and 0.028-2.75 g kg^{-1}

264   coal, respectively (Chen et al., 2005; Zhang et al., 2008). The emission factors of various

265   pollutants from a typical residential coal stove fueled with raw bituminous coal were also

266   investigated in our group (Du et al., 2016; Liu et al., 2017) according to farmers' customary uses

267   of coal stoves under the alternation cycles of flaming and smoldering. The emission factors of OC

268   and EC under the entire combustion process could achieve to be 10.99 $\pm$ 0.95 g kg^{-1} coal and 0.84

269    $\pm$ 0.06 g kg^{-1} coal, respectively (Table 3). Considering the high density of farmers in the rural area,

270   the largest levels of atmospheric OC and EC at DBT could be rationally ascribed to residential

271   coal combustion. However, the proportion of the WSIs from residential coal combustion (Fig. 7a)

272   were extremely low with respect to that of the atmosphere. Therefore, the largest levels of the key

273   WSIs in PM$_{2.5}$ at DBT were suspected to the secondary formation via the heterogeneous or

274   multiphase reactions which might be accelerated by the OC and EC particles (Han et al., 2013;

275   Zhao et al., 2016) emitted from residential coal combustion.

276   Although the three sampling sites of DBT, WD and BD are closely adjacent, the lowest

277   concentrations of the key species in PM$_{2.5}$ were observed at WD, which was probably ascribed to

278   the replacement of coal with natural gas for the central heating in the county of WD (a main pipe

279   of natural gas is just across the county), e.g., the average concentration of NO$_2$ was higher at WD

280   than at BD, whereas the average concentration of SO$_2$ was on the contrary (Table 2).

281   The city of BD and the county of WD are fully surrounded by high density of countryside,

282   whereas the city of BJ is only neighbored with high density of countryside in the

283   south-southeast-southwest directions, and thus the residential coal combustion was also suspected

284 to be responsible for the remarkably higher concentrations of the key species in $PM_{2.5}$ at BD and

285 WD than at BJ. To confirm the above assumptions, the chemical composition and source

286 characteristics of the species in $PM_{2.5}$ were further analyzed in the following section.

287 **3.3 Chemical composition of $PM_{2.5}$ at the four sampling sites**

288 The average mass proportions of the species in $PM_{2.5}$ during the sampling period at the four

289 sampling sites are illustrated in Fig. 7b. OC, EC, NH_4^+, NO_3^- and SO_4^{2-} were found to be the

290 principal species, accounting for about 82 %-88 % of the total species in $PM_{2.5}$ at each sampling

291 site, which were in line with previous studies (Zhao et al., 2013a; X. J. Zhao et al., 2013; Tian et

292 al., 2014; Huang et al., 2014). As for the proportions of individual species, there were obvious

293 differences between the sampling site of BJ and the sampling sites of BD, WD and DBT. The

294 average mass proportions of OC and EC at BD, WD and DBT were very close, accounting for

295 about 45.7 %-47.1 % and 9.0 %-10.4 % of the total species in $PM_{2.5}$, respectively, which were

296 about 8 % for OC and 2 % for EC greater than those at BJ. In contrast to OC and EC, the average

297 mass proportions of NO_3^- (10.1 %-10.8 %) and SO_4^{2-} (11.2 %-11.7 %) at BD, WD and DBT were

298 about 5 % and 3 % less than those (15.1 % for NO_3^- and 14.0 % for SO_4^{2-}) at BJ, respectively. The

299 obvious differences of the mass proportions of OC, EC, NO_3^- and SO_4^{2-} between the sampling site

300 of BJ and the sampling sites of BD, WD and DBT indicated that the sources for the principal

301 species at BJ were different from the other three sampling sites. The mass proportions of OC, EC,

302 NO_3^- and SO_4^{2-} at BD and WD were very close to those at DBT, implying that residential coal

303 combustion might also be the dominant source for the species in $PM_{2.5}$ at BD and WD. Residential

304 sector (dominated by residential coal combustion) in the region of BTH during winter has been

305 recognized as the dominant source for atmospheric OC and EC (Chen et al., 2017), which was

306   estimated to contribute 85% and 65% of primary OC and EC emissions, respectively (J. Liu et al.,

307   2016). Because the sampling sites of DBT, BD and WD are located in or fully surrounded by high

308   density of countryside, the contribution of residential coal combustion to atmospheric OC and EC

309   at DBT, BD and WD must evidently exceed the regional values estimated by J. Liu et al. (2016).

310   Although the mass proportions of NO_3^- and SO_4^{2-} were evidently lower at BD, WD and DBT than

311   at BJ, the average mass concentrations of NO_3^- and SO_4^{2-} were on the contrary (Table 2).

312   Atmospheric NO_3^- and SO_4^{2-} are mainly from secondary formation via heterogeneous, multiphase

313   or gas-phase reactions which are depended on the concentrations of their precursors (NO_2 and SO_2)

314   and OH radicals, the surface characteristics and areas of particles, and RH (Ravishankara, 1997;

315   Wang et al., 2013; Quan et al., 2014; Nie et al., 2014; He et al., 2014; Yang et al., 2015; B. Zheng

316   et al., 2015). The remarkably higher concentrations of NO_2, SO_2 and $PM_{2.5}$ at BD, WD and DBT

317   (Liu et al., 2015) than at BJ (Table 2) favored secondary formation of NO_3^- and SO_4^{2-}, resulting in

318   the relatively high concentrations of NO_3^- and SO_4^{2-}.

319   As shown in Fig. 8, the serious pollution episodes at BJ usually occurred during the periods with

320   the air parcel from the southwest-south directions where farmers with high density reside, and thus

321   residential coal combustion might also make evident contribution to atmospheric pollutants at BJ.

322   Because the species in $PM_{2.5}$ at BJ during the serious pollution episodes accounted for very large

323   weight of their average concentrations, the proportions of the species in $PM_{2.5}$ were dominated by

324   the serious pollution events. The highest NO_3^- and SO_4^{2-} proportions and the lowest OC and EC

325   proportions at BJ among the four sampling sites might be partly ascribed to the conversions of

326   NO_2 and SO_2 to NO_3^- and SO_4^{2-} during the air parcel transportation from the south-southwest

327   directions. The contribution of the transportation to atmospheric OC and EC at BJ could be

328   verified by the correlations between the OC/EC ratios and the $PM_{2.5}$ levels (Fig. 9). The OC/EC

329   ratios (about 4.9 ± 0.7) at WD and DBT were almost independent of the $PM_{2.5}$ levels, whereas the

330   OC/EC ratios at BJ and BD remarkably decreased with increasing the $PM_{2.5}$ levels and reached the

331   almost same value (about 4.8 ± 0.5) as those at WD and DBT when the concentrations of $PM_{2.5}$

332   were above 150 μg m^{-3} (the serious pollution events). Because there were relatively sparse

333   emissions from vehicles and industries at WD and DBT, the almost constant of OC/EC ratios

334   under the different levels of $PM_{2.5}$ at WD and DBT further revealed that atmospheric OC and EC

335   were dominated by the local residential coal combustion. The almost same OC/EC ratios at the

336   four sampling sites with the concentrations of $PM_{2.5}$ greater than 150 μg m^{-3} indicated that the

337   residential coal combustion also made dominant contribution to atmospheric OC and EC in the

338   two cities during the severe pollution period. Our previous study (C. Liu et al., 2016) also found

339   that the contribution from residential coal combustion to atmospheric VOCs increased from 23 %

340   to 33 % with increasing pollution levels in Beijing.

341   It should be mentioned that the OC/EC ratios observed at DBT and WD were about a factor of 2.7

342   less than that (13.1) of the emission from the residential coal combustion, whereas at BJ and BD

343   were too high to be explained by direct emissions from diesel (0.4-0.8) and gasoline (3.1) vehicles

344   (Shah et al., 2004; Geller et al., 2006). The OC emitted from the residential coal combustion might

345   be easily degraded or volatilized in the atmosphere, resulting in the relatively low OC/EC ratios

346   observed at DBT and WD. In China, aromatic compounds as typical pollutants from vehicle

347   emissions are very reactive to make contribution to secondary organic aerosols (SOA) (Zhang et

348   al., 2017), which was suspected to make evident contribution to the OC/EC ratios at BJ and BD

349   when the atmospheric EC concentrations were relatively low. For example, the extremely high

350 OC/EC ratios (> 6.0) at BJ and BD only occurred when the atmospheric EC concentrations were

351 less than 3.2 μg m^{-3} at BJ and 5.4 μg m^{-3} at BD. Because the atmospheric EC concentrations at BJ

352 and BD were about a factor of 4-6 greater during the serious pollution events than during the

353 slight pollution events, the effect of SOA formation on the OC/EC ratios would become less

354 during the serious pollution events if the SOA formation rate kept constant.

355 **3.4 Correlations among the species in PM$_{2.5}$**

356 The correlations among the WSIs, OC and EC in PM$_{2.5}$ at the four sampling sites are listed in

357 Table 4. The number of the species involved in significant correlations evidently increased from

358 the countryside to the cities and was 18, 28, 30 and 36 at DBT, WD, BD and BJ, respectively. The

359 significant correlations among the species could be classified as three types: 1) associated with OC

360 and EC; 2) associated with Ca^{2+} and Mg^{2+}; and 3) associated with K^{+}. Three types of significant

361 correlations at DBT were independent of each other, whereas they were involved in interrelation

362 more and more from WD to BJ. The independence for the three types of significant correlations at

363 DBT further confirmed that residential coal combustion was preferentially dominant source for

364 atmospheric OC and EC. The significant correlations among OC, EC, NO$_3^-$, NH$_4^+$ and Cl$^-$ at DBT

365 indicated that the OC and EC emitted from the residential coal combustion could quickly

366 accelerate secondary formation of NO$_3^-$, NH$_4^+$ and Cl$^-$ via heterogeneous or multiphase reactions

367 of NO$_x$, NH$_3$ and HCl which have been verified to be emitted from the residential coal combustion

368 (Wang et al., 2005; Shapiro et al., 2007; Bläsing and Müller, 2010; Meng et al., 2011; Zhang et al.,

369 2013; Gao et al., 2015; Li et al., 2016a; Huang et al., 2016). The interrelation for the three types of

370 significant correlations at WD, BD and BJ implied that complex sources including local emissions

371 and regional transportation were dominant for atmospheric species in the cities. The species

372   associated with Ca^{2+} and Mg^{2+} from construction and road dust (Liang et al., 2016) as well as the

373   species associated with K^+ from biomass (municipal solid waste) burning (Gao et al., 2011; J. Li et

374   al., 2014; Yao et al., 2016) in the cities would accumulate under stagnant air conditions at the earth

375   surface, meanwhile the OC and EC concentrations could also increase due to the air parcel

376   transportation with abundant OC and EC in the upper layer from the south-southwest directions

377   (Fig. 8). It is interesting to note that the significant correlations among OC, EC, NO_3^-, NH_4^+ and

378   Cl^- were found at the four sampling sites, whereas the significant correlation between OC (or EC)

379   and SO_4^{2-} was only found at BJ. Because the sampling sites of DBT, WD and BD are close to the

380   source of OC and EC from the residential coal combustion, the significant correlations among OC,

381   EC, NO_3^-, NH_4^+ and Cl^- but the insignificant correlation between OC (or EC) and SO_4^{2-} implied

382   that the formation rate of SO_4^{2-} via heterogeneous or multiphase reactions might be relatively

383   slower than those of NO_3^-, NH_4^+ and Cl^-. The reactive uptake coefficients of SO_2 oxidation by O_3

384   were reported to be from 4.3×10^{-8} to 7×10^{-7} on different mineral aerosols and from 1×10^{-6} to

385   6×10^{-6} on soot particles (Wu et al., 2011; Song et al., 2012), which were at least one order of

386   magnitude less than those of NO_2 (1.03×10^{-2}-3.43×10^{-3} on soot particles and 1.03×10^{-6}-1.2×10^{-5}

387   on mineral aerosols) (Underwood et al., 2001; Esteve et al., 2004; Ma et al., 2011; Ma et al., 2017).

388   The OC, EC and SO_2 emitted from the residential coal combustion experienced the relatively long

389   period of excursion to be transported to Beijing, resulting in the significant correlation between

390   OC (or EC) and SO_4^{2-} at BJ.

391   As listed in Table 5, the pronounced correlations for [As] vs. [Se] and [Cu] vs. [Zn] at the four

392   sampling sites indicated that the two pairs of elements were from the common sources. Based on

393   the remarkable elevations of As and Se near a coal-fired power plant with respect to the

17

394   background site, Jayasekher (2009) pointed out that their significant correlation can be used as the

395   tracer for coal combustion. Because Cu and Zn have been found to be mainly released from the

396   additives of vehicle lubricating oils, brake and tire wear during transportation activities (Yu et al.,

397   2013; Zhang et al., 2013; Tan et al., 2016), their significant correlation has been used as the tracer

398   for vehicle emissions. Both coal combustion and vehicle emissions could make contribution to

399   atmospheric Pb (Zhang et al., 2013; Gao et al., 2016), and thus the correlations for [Pb] vs.

400   [Cu+Zn] and [Pb] vs. [As+Se] could reflect their local dominant sources. As shown in Fig. 10, the

401   significant correlation between [Pb] and [Cu+Zn] but no correlation between [Pb] and [As+Se]

402   were found at BJ, whereas the correlations at the rural site of DBT were on the contrary, indicating

403   that atmospheric Pb, Cu and Zn at BJ were mainly related to the vehicle emissions and

404   atmospheric Pb, As and Se at DBT were dominated by residential coal combustion. Because the

405   sampling sites of BD and WD were affected by both vehicle emissions and residential coal

406   combustion, the significant correlations between [Pb] and [Cu+Zn] as well as [Pb] and [As+Se]

407   were found at the two sampling sites. Although there was no correlation between [Pb] and [As+Se]

408   at BJ, the contribution of residential coal combustion to atmospheric $PM_{2.5}$ in the city of BJ could

409   not be excluded because the trace elements from coal combustion are mainly present in relatively

410   large particles (0.8-2.5 μm) which might quickly deposit near their sources (Wang et al., 2008).

411   **3.5 Source apportionment of $PM_{2.5}$ at the four sampling sites**

412   The source characteristics of $PM_{2.5}$ at the four sampling sites were analyzed by the CMC method

413   which has been described in detail in section 2.3. The average proportions of the species from

414   different sources in $PM_{2.5}$ during the sampling period at the four sampling sites are comparatively

415   shown in Fig. 11. It is evident that secondary aerosols (SIA + SOC) accounted for the largest

416   proportion (about 32-41 %) in $PM_{2.5}$, followed by POC (about 24-28 %), EC (about 6-8 %),

417   mineral dust (about 2-8 %) and Cl^-_{cc} (about 2-5 %) at the four sampling sites. The proportion of

418   mineral dust was the highest at BJ and the lowest at DBT among the four sampling sites, whereas

419   the proportion of Cl^-_{cc} was on the contrary. Because the concentrations of the mineral dust

420   compounds were much higher under stagnant weather condition than under clean days at BJ, the

421   remarkably high proportion of mineral dust at BJ was mainly ascribed to the emissions from road

422   dust and construction (Liang et al., 2016) during the sampling period. The obviously high

423   proportion of Cl^-_{cc} at DBT was ascribed to the emission from residential coal combustion (Shen et

424   al., 2016). In addition, the proportions of TEO, K^+_{bb} and Cl^-_{ss} were less than about 2 %, which

425   were insignificant to the sources of $PM_{2.5}$ at the four sampling sites during the sampling period.

426   Atmospheric Primary Organic Matters (POM) and Cl^-_{cc} at the four sampling sites could be

427   estimated based on POM≈POC × 1.6 (Cheung et al., 2005; Hsu et al., 2010b; Han et al., 2015)

428   and the formulas (1)-(4), respectively. The sum of POM, EC and Cl^-_{cc} at DBT was assumed to be

429   solely from residential coal combustion, accounting for about 58% in $PM_{2.5}$ (Fig. 12). Assuming

430   that the ratio of Cl^-_{cc} to the sum of POM, EC and Cl^-_{cc} was constant for coal combustion at the four

431   sampling sites, the primary contribution of coal combustion to atmospheric $PM_{2.5}$ at BJ, BD and

432   WD could be estimated to be 32 %, 49 % and 43 % (Fig. 12), respectively. The annual residential

433   coal consumption mainly focused on the four months in winter, accounting for about 11 % of the

434   total coal consumption in the region of BTH. Because the emission factor of $PM_{2.5}$ from

435   residential coal combustion (about 1054-12910 mg kg^{-1}) was about 1-3 orders of magnitude

436   greater than those from industry boilers or coal power plants (about 16-100 mg kg^{-1}) (Chen et al.,

437   2005; Zhang et al., 2008), the estimated proportions of the contribution of coal combustion to

438   atmospheric $PM_{2.5}$ at the four sampling sites during the winter were mainly ascribed to residential

439   coal combustion. If only the primary $PM_{2.5}$ was considered, the contribution of residential coal

440   combustion to the primary $PM_{2.5}$ at BJ would achieve to be about 59 % which was in line with the

441   value of 57 % estimated by J. Liu et al. (2016) for the winter of 2010 in Beijing.

442   **4 Conclusions**

443   Based on the comprehensive analysis of the levels, composition characteristics, the correlations of

444   the key species in $PM_{2.5}$ and the back trajectories, residential coal combustion in the North China

445   during winter was found not only to be the dominant source for atmospheric OC, EC, Cl^-, NO_3^-,

446   SO_4^{2-} and NH_4^+ in rural areas but also to make evident contribution to the species in cities.

447   According to the CMC method, the contributions of the primary particle emission from residential

448   coal combustion to atmospheric $PM_{2.5}$ at BJ, BD, WD and DBT during winter were estimated to

449   be 32 %, 49 %, 43 % and 58 %, respectively. Therefore, strict control measures should be

450   implemented for the emissions from residential coal combustion to mitigate the currently serious

451     $PM_{2.5}$ pollution during the winter in the North China.

452   **Author contribution**

453   **Y. J. Mu** designed the experiments and prepared the manuscript. **P. F. Liu** and **C. L. Zhang**

454   carried out the experiments and prepared the manuscript, and contributed equally to this work. **C.**

455   **Y. Xue** carried out the experiments. **J. F. Liu**, **Y. Y. Zhang**, **D. Tian** and **C. Ye** were involved in

456   part of the work. **H. X. Zhang** provided the meteorological data and trace gases in Beijing. **J.**

457   **Guan** provided the meteorological data and trace gases in Baoding and Wangdu.

458   **Acknowledgements**

20

464   **References**

465   Bläsing, M., and Müller, M.: Mass spectrometric investigations on the release of inorganic species
466   during gasification and combustion of German hard coals, Combustion and Flame, 157,
467   1374-1381, 10.1016/j.combustflame.2010.01.003, 2010.

468   Bläsing, M., and Müller, M.: Release of Alkali Metal, Sulfur, and Chlorine Species during
469   High-Temperature Gasification of Coal and Coal Blends in a Drop Tube Reactor, Energy & Fuels,
470   26, 6311-6315, 10.1021/ef301205j, 2012.

471   Brewer, P. G. (Eds.): Minor elements in sea water, Chemical Oceanography, Academic, San Diego,
472   California, 1975.

473   Buseck, P. R., and Posfai, M.: Airborne minerals and related aerosol particles: Effects on climate
474   and the environment, Proceedings of the National Academy of Sciences of the United States of
475   America, 96, 3372-3379, 10.1073/pnas.96.7.3372, 1999.

476   Chan, C. K., and Yao, X.: Air pollution in mega cities in China, Atmospheric Environment, 42,
477   1-42, 10.1016/j.atmosenv.2007.09.003, 2008.

478   Chen, C., Sun, Y. L., Xu, W. Q., Du, W., Zhou, L. B., Han, T. T., Wang, Q. Q., Fu, P. Q., Wang, Z.
479   F., Gao, Z. Q., Zhang, Q., and Worsnop, D. R.: Characteristics and sources of submicron aerosols
480   above the urban canopy (260 m) in Beijing, China, during the 2014 APEC summit, Atmospheric
481   Chemistry and Physics, 15, 12879-12895, 10.5194/acp-15-12879-2015, 2015.

482   Chen, L. H., Sun, Y. Y., Wu, X. C., Zhang, Y. X., Zheng, C. H., Gao, X., and Cen, K.: Unit-based
483   emission inventory and uncertainty assessment of coal-fired power plants, Atmospheric
484   Environment, 99, 527-535, 10.1016/j.atmosenv.2014.10.023, 2014.

485   Chen, S., Xu, L., Zhang, Y., Chen, B., Wang, X., Zhang, X., Zheng, M., Chen, J., Wang, W., Sun,
486   Y., Fu, P., Wang, Z., and Li, W.: Direct observations of organic aerosols in common wintertime
487   hazes in North China: insights into direct emissions from Chinese residential stoves, Atmospheric
488   Chemistry and Physics, 17, 1259-1270, 10.5194/acp-17-1259-2017, 2017.

489   Chen, Y. J., Sheng, G. Y., Bi, X. H., Feng, Y. L., Mai, B. X., and Fu, J. M.: Emission factors for
490   carbonaceous particles and polycyclic aromatic hydrocarbons from residential coal combustion in
491   China, Environ. Sci. Technol., 39, 1861-1867, 10.1021/es0493650, 2005.

492   Cheng, Y., He, K. B., Duan, F. K., Zheng, M., Du, Z. Y., Ma, Y. L., and Tan, J. H.: Ambient
493   organic carbon to elemental carbon ratios: Influences of the measurement methods and
494   implications, Atmospheric Environment, 45, 2060-2066, 10.1016/j.atmosenv.2011.01.064, 2011.

495   Cheng, Y., Zheng, G., Wei, C., Mu, Q., Zheng, B., Wang, Z., Gao, M., Zhang, Q., He, K.,
496   Carmichael, G., Pöschl, U., and Su, H.: Reactive nitrogen chemistry in aerosol water as a source
497   of sulfate during haze events in China, Science Advances, 2, 10.1126/sciadv.1601530, 2016.

498   Cheng, Y. F., Eichler, H., Wiedensohler, A., Heintzenberg, J., Zhang, Y. H., Hu, M., Herrmann, H.,

499   Zeng, L. M., Liu, S., Gnauk, T., Brüggemann, E., and He, L. Y.: Mixing state of elemental carbon
500   and non-light-absorbing aerosol components derived from in situ particle optical properties at
501   Xinken in Pearl River Delta of China, Journal of Geophysical Research, 111,
502   10.1029/2005jd006929, 2006.

503   Cheung, H. C., Wang, T., Baumann, K., and Guo, H.: Influence of regional pollution outflow on
504   the concentrations of fine particulate matter and visibility in the coastal area of southern China,
505   Atmospheric Environment, 39, 6463-6474, 10.1016/j.atmosenv.2005.07.033, 2005.

506   Cui, H., Mao, P., Zhao, Y., Nielsen, C. P., and Zhang, J.: Patterns in atmospheric carbonaceous
507   aerosols in China: emission estimates and observed concentrations, Atmospheric Chemistry and
508   Physics, 15, 8657-8678, 10.5194/acp-15-8657-2015, 2015.

509   Ding, X., Wang, X. M., Gao, B., Fu, X. X., He, Q. F., Zhao, X. Y., Yu, J. Z., and Zheng, M.:
510   Tracer-based estimation of secondary organic carbon in the Pearl River Delta, south China,
511   Journal of Geophysical Research: Atmospheres, 117, D05313, 10.1029/2011jd016596, 2012.

512   Du, Q., Zhang, C., Mu, Y., Cheng, Y., Zhang, Y., Liu, C., Song, M., Tian, D., Liu, P., Liu, J., Xue,
513   C., and Ye, C.: An important missing source of atmospheric carbonyl sulfide: Domestic coal
514   combustion, Geophysical Research Letters, 43, 8720-8727, 10.1002/2016gl070075, 2016.

515   Duan, J., Tan, J., Wang, S., Chai, F., He, K., and Hao, J.: Roadside, Urban, and Rural comparison
516   of size distribution characteristics of PAHs and carbonaceous components of Beijing, China,
517   Journal of Atmospheric Chemistry, 69, 337-349, 10.1007/s10874-012-9242-5, 2012.

518   Esteve, W., Budzinski, H., and Villenave, E.: Relative rate constants for the heterogeneous
519   reactions of OH, NO_2 and NO radicals with polycyclic aromatic hydrocarbons adsorbed on
520   carbonaceous particles. Part 1: PAHs adsorbed on 1–2μm calibrated graphite particles,
521   Atmospheric Environment, 38, 6063-6072, 10.1016/j.atmosenv.2004.05.059, 2004.

522   Gao, J., Tian, H., Cheng, K., Lu, L., Zheng, M., Wang, S., Hao, J., Wang, K., Hua, S., Zhu, C., and
523   Wang, Y.: The variation of chemical characteristics of $PM_{2.5}$ and PM_{10} and formation causes
524   during two haze pollution events in urban Beijing, China, Atmospheric Environment, 107, 1-8,
525   10.1016/j.atmosenv.2015.02.022, 2015.

526   Gao, J., Peng, X., Chen, G., Xu, J., Shi, G. L., Zhang, Y. C., and Feng, Y. C.: Insights into the
527   chemical characterization and sources of $PM_{2.5}$ in Beijing at a 1-h time resolution, The Science of
528   the total environment, 542, 162-171, 10.1016/j.scitotenv.2015.10.082, 2016.

529   Gao, M., Carmichael, G. R., Wang, Y., Saide, P. E., Yu, M., Xin, J., Liu, Z., and Wang, Z.:
530   Modeling study of the 2010 regional haze event in the North China Plain, Atmospheric Chemistry
531   and Physics, 16, 1673-1691, 10.5194/acp-16-1673-2016, 2016.

532   Gao, X., Yang, L., Cheng, S., Gao, R., Zhou, Y., Xue, L., Shou, Y., Wang, J., Wang, X., Nie, W.,
533   Xu, P., and Wang, W.: Semi-continuous measurement of water-soluble ions in $PM_{2.5}$ in Jinan,
534   China: Temporal variations and source apportionments, Atmospheric Environment, 45, 6048-6056,
535   10.1016/j.atmosenv.2011.07.041, 2011.

536   Geller, M. D., Ntziachristos, L., Mamakos, A., Samaras, Z., Schmitz, D. A., Froines, J. R., and
537   Sioutas, C.: Physicochemical and redox characteristics of particulate matter (PM) emitted from
538   gasoline and diesel passenger cars, Atmospheric Environment, 40, 6988-7004,
539   10.1016/j.atmosenv.2006.06.018, 2006.

540   Geng, C., Chen, J., Yang, X., Ren, L., Yin, B., Liu, X., and Bai, Z.: Emission factors of polycyclic
541   aromatic hydrocarbons from domestic coal combustion in China, Journal of Environmental
542   Sciences, 26, 160-166, 10.1016/s1001-0742(13)60393-9, 2014.

543 Guo, S., Hu, M., Zamora, M. L., Peng, J., Shang, D., Zheng, J., Du, Z., Wu, Z., Shao, M., Zeng, L.,
544 Molina, M. J., and Zhang, R.: Elucidating severe urban haze formation in China, Proceedings of
545 the National Academy of Sciences of the United States of America, 111, 17373-17378,
546 10.1073/pnas.1419604111, 2014.

547 Han, C., Liu, Y., and He, H.: Role of organic carbon in heterogeneous reaction of NO_2 with soot,
548 Environ Sci Technol, 47, 3174-3181, 10.1021/es304468n, 2013.

549 Han, T., Liu, X., Zhang, Y., Qu, Y., Zeng, L., Hu, M., and Zhu, T.: Role of secondary aerosols in
550 haze formation in summer in the Megacity Beijing, J Environ Sci (China), 31, 51-60,
551 10.1016/j.jes.2014.08.026, 2015.

552 He, H., Wang, Y., Ma, Q., Ma, J., Chu, B., Ji, D., Tang, G., Liu, C., Zhang, H., and Hao, J.:
553 Mineral dust and NO_x promote the conversion of SO_2 to sulfate in heavy pollution days, Scientific
554 reports, 4, 4172, 10.1038/srep04172, 2014.

555 He, Y., Qiu, K. Z., Whiddon, R., Wang, Z. H., Zhu, Y. Q., Liu, Y. Z., Li, Z. S., and Cen, K. F.:
556 Release characteristic of different classes of sodium during combustion of Zhun-Dong coal
557 investigated by laser-induced breakdown spectroscopy, Science Bulletin, 60, 1927-1934, 2015.

558 Ho, K. F., Lee, S. C., Cao, J. J., Chow, J. C., Watson, J. G., and Chan, C. K.: Seasonal variations
559 and mass closure analysis of particulate matter in Hong Kong, The Science of the total
560 environment, 355, 276-287, 10.1016/j.scitotenv.2005.03.013, 2006.

561 Hsu, S. C., Liu, S. C., Arimoto, R., Shiah, F. K., Gong, G. C., Huang, Y. T., Kao, S. J., Chen, J. P.,
562 Lin, F. J., Lin, C. Y., Huang, J. C., Tsai, F., and Lung, S. C. C.: Effects of acidic processing,
563 transport history, and dust and sea salt loadings on the dissolution of iron from Asian dust, Journal
564 of Geophysical Research, 115, 10.1029/2009jd013442, 2010a.

565 Hsu, S. C., Liu, S. C., Tsai, F., Engling, G., Lin, I. I., Chou, C. K. C., Kao, S. J., Lung, S. C. C.,
566 Chan, C. Y., Lin, S. C., Huang, J. C., Chi, K. H., Chen, W. N., Lin, F. J., Huang, C. H., Kuo, C. L.,
567 Wu, T. C., and Huang, Y. T.: High wintertime particulate matter pollution over an offshore island
568 (Kinmen) off southeastern China: An overview, Journal of Geophysical Research, 115,
569 10.1029/2009jd013641, 2010b.

570 Huang, R. J., Zhang, Y., Bozzetti, C., Ho, K. F., Cao, J. J., Han, Y., Daellenbach, K. R., Slowik, J.
571 G., Platt, S. M., Canonaco, F., Zotter, P., Wolf, R., Pieber, S. M., Bruns, E. A., Crippa, M., Ciarelli,
572 G., Piazzalunga, A., Schwikowski, M., Abbaszade, G., Schnelle-Kreis, J., Zimmermann, R., An, Z.,
573 Szidat, S., Baltensperger, U., El Haddad, I., and Prevot, A. S.: High secondary aerosol contribution
574 to particulate pollution during haze events in China, Nature, 514, 218-222, 10.1038/nature13774,
575 2014.

576 Huang, X., Liu, Z., Zhang, J., Wen, T., Ji, D., and Wang, Y.: Seasonal variation and secondary
577 formation of size-segregated aerosol water-soluble inorganic ions during pollution episodes in
578 Beijing, Atmospheric Research, 168, 70-79, 10.1016/j.atmosres.2015.08.021, 2016.

579 Jayasekher, T.: Aerosols near by a coal fired thermal power plant: chemical composition and toxic
580 evaluation, Chemosphere, 75, 1525-1530, 10.1016/j.chemosphere.2009.02.001, 2009.

581 Kong, S. F., Li, L., Li, X. X., Yin, Y., Chen, K., Liu, D. T., Yuan, L., Zhang, Y. J., Shan, Y. P., and
582 Ji, Y. Q.: The impacts of firework burning at the Chinese Spring Festival on air quality: insights of
583 tracers, source evolution and aging processes, Atmospheric Chemistry and Physics, 15, 2167-2184,
584 10.5194/acp-15-2167-2015, 2015.

585 Landis, M. S., Norris, G. A., Williams, R. W., and Weinstein, J. P.: Personal exposures to $PM_{2.5}$
586 mass and trace elements in Baltimore, MD, USA, Atmospheric Environment, 35, 6511-6524,

10.1016/s1352-2310(01)00407-1, 2001.

Li, J., Song, Y., Mao, Y., Mao, Z., Wu, Y., Li, M., Huang, X., He, Q., and Hu, M.: Chemical characteristics and source apportionment of $PM_{2.5}$ during the harvest season in eastern China's agricultural regions, Atmospheric Environment, 92, 442-448, 10.1016/j.atmosenv.2014.04.058, 2014.

Li, Q., Jiang, J. K., Cai, S. Y., Zhou, W., Wang, S. X., Duan, L., and Hao, J. M.: Gaseous Ammonia Emissions from Coal and Biomass Combustion in Household Stoves with Different Combustion Efficiencies, Environmental Science & Technology Letters, 3, 98-103, 10.1021/acs.estlett.6b00013, 2016a.

Li, Q., Li, X., Jiang, J., Duan, L., Ge, S., Zhang, Q., Deng, J., Wang, S., and Hao, J.: Semi-coke briquettes: towards reducing emissions of primary $PM_{2.5}$, particulate carbon, and carbon monoxide from household coal combustion in China, Scientific reports, 6, 19306, 10.1038/srep19306, 2016b.

Li, T., Wang, Y., Li, W. J., Chen, J. M., Wang, T., and Wang, W. X.: Concentrations and solubility of trace elements in fine particles at a mountain site, southern China: regional sources and cloud processing, Atmospheric Chemistry and Physics, 15, 8987-9002, 10.5194/acp-15-8987-2015, 2015.

Li, W., Wang, C., Wang, H., Chen, J., Yuan, C., Li, T., Wang, W., Shen, H., Huang, Y., Wang, R., Wang, B., Zhang, Y., Chen, H., Chen, Y., Tang, J., Wang, X., Liu, J., Coveney, R. M., Jr., and Tao, S.: Distribution of atmospheric particulate matter (PM) in rural field, rural village and urban areas of northern China, Environ Pollut, 185, 134-140, 10.1016/j.envpol.2013.10.042, 2014.

Li, Y., Ye, C., Liu, J., Zhu, Y., Wang, J., Tan, Z., Lin, W., Zeng, L., and Zhu, T.: Observation of regional air pollutant transport between the megacity Beijing and the North China Plain, Atmospheric Chemistry and Physics, 16, 14265-14283, 10.5194/acp-16-14265-2016, 2016.

Liang, C. S., Duan, F. K., He, K. B., and Ma, Y. L.: Review on recent progress in observations, source identifications and countermeasures of $PM_{2.5}$, Environ Int, 86, 150-170, 10.1016/j.envint.2015.10.016, 2016.

Liu, C., Mu, Y., Liu, J., Zhang, C., Zhang, Y., Liu, P., and Zhang, H.: The levels, variation characteristics and sources of atmospheric non-methane hydrocarbon compounds during wintertime in Beijing, China, Atmos. Chem. Phys. Discuss., 2016, 1-23, 10.5194/acp-2016-783, 2016.

Liu, C., Zhang, C., Mu, Y., Liu, J., and Zhang, Y.: Emission of volatile organic compounds from domestic coal stove with the actual alternation of flaming and smoldering combustion processes, Environ Pollut, 221, 385-391, 10.1016/j.envpol.2016.11.089, 2017.

Liu, J., Mauzerall, D. L., Chen, Q., Zhang, Q., Song, Y., Peng, W., Klimont, Z., Qiu, X. H., Zhang, S. Q., Hu, M., Lin, W. L., Smith, K. R., and Zhu, T.: Air pollutant emissions from Chinese households: A major and underappreciated ambient pollution source, Proceedings of the National Academy of Sciences of the United States of America, 113, 7756-7761, 10.1073/pnas.1604537113, 2016.

Liu, K., Zhang, C., Cheng, Y., Liu, C., Zhang, H., Zhang, G., Sun, X., and Mu, Y.: Serious BTEX pollution in rural area of the North China Plain during winter season, J Environ Sci (China), 30, 186-190, 10.1016/j.jes.2014.05.056, 2015.

Liu, P., Zhang, C., Mu, Y., Liu, C., Xue, C., Ye, C., Liu, J., Zhang, Y., and Zhang, H.: The possible contribution of the periodic emissions from farmers' activities in the North China Plain to

atmospheric water-soluble ions in Beijing, Atmospheric Chemistry and Physics, 16, 10097-10109, 10.5194/acp-16-10097-2016, 2016.

Ma, J., Liu, Y., and He, H.: Heterogeneous reactions between NO_2 and anthracene adsorbed on SiO_2 and MgO, Atmospheric Environment, 45, 917-924, 10.1016/j.atmosenv.2010.11.012, 2011.

Ma, Q., Wang, T., Liu, C., He, H., Wang, Z., Wang, W., and Liang, Y.: SO_2 Initiates the Efficient Conversion of NO_2 to HONO on MgO Surface, Environ. Sci. Technol., 51, 3767-3775, 10.1021/acs.est.6b05724, 2017.

Ma, Z. W., Hu, X. F., Sayer, A. M., Levy, R., Zhang, Q., Xue, Y. G., Tong, S. L., Bi, J., Huang, L., and Liu, Y.: Satellite-Based Spatiotemporal Trends in $PM_{2.5}$ Concentrations: China, 2004-2013, Environ. Health Perspect., 124, 184-192, 10.1289/ehp.1409481, 2016.

Mantas, E., Remoundaki, E., Halari, I., Kassomenos, P., Theodosi, C., Hatzikioseyian, A., and Mihalopoulos, N.: Mass closure and source apportionment of $PM_{2.5}$ by Positive Matrix Factorization analysis in urban Mediterranean environment, Atmospheric Environment, 94, 154-163, 10.1016/j.atmosenv.2014.05.002, 2014.

Meng, Z. Y., Lin, W. L., Jiang, X. M., Yan, P., Wang, Y., Zhang, Y. M., Jia, X. F., and Yu, X. L.: Characteristics of atmospheric ammonia over Beijing, China, Atmospheric Chemistry and Physics, 11, 6139-6151, 10.5194/acp-11-6139-2011, 2011.

Nel, A.: Air pollution-related illness: Effects of particles, Science, 308, 804-806, 10.1126/science.1108752, 2005.

Nie, W., Ding, A., Wang, T., Kerminen, V. M., George, C., Xue, L., Wang, W., Zhang, Q., Petaja, T., Qi, X., Gao, X., Wang, X., Yang, X., Fu, C., and Kulmala, M.: Polluted dust promotes new particle formation and growth, Scientific reports, 4, 6634, 10.1038/srep06634, 2014.

Peplow, M.: Beijing smog contains witches' brew of microbes, Nature, doi, 10, 2014.

Poschl, U.: Atmospheric aerosols: composition, transformation, climate and health effects, Angew Chem Int Ed Engl, 44, 7520-7540, 10.1002/anie.200501122, 2005.

Quan, J., Tie, X., Zhang, Q., Liu, Q., Li, X., Gao, Y., and Zhao, D.: Characteristics of heavy aerosol pollution during the 2012–2013 winter in Beijing, China, Atmospheric Environment, 88, 83-89, 10.1016/j.atmosenv.2014.01.058, 2014.

Ravishankara, A.: Heterogeneous and multiphase chemistry in the troposphere, Science, 276, 1058-1065, 1997.

Revuelta, C. C., de la Fuente Santiago, E., and Vázquez, J. A. R.: Characterization of Polycyclic Aromatic Hydrocarbons in Emissions from Coal-Fired Power Plants: The Influence of Operation Parameters, Environmental Technology, 20, 61-68, 10.1080/09593332008616793, 1999.

Shah, S. D., Cocker, D. R., Miller, J. W., and Norbeck, J. M.: Emission Rates of Particulate Matter and Elemental and Organic Carbon from In-Use Diesel Engines, Environ. Sci. Technol., 38, 2544-2550, 10.1021/es0350583, 2004.

Shapiro, J. B., Simpson, H. J., Griffin, K. L., and Schuster, W. S. F.: Precipitation chloride at West Point, NY: Seasonal patterns and possible contributions from non-seawater sources, Atmospheric Environment, 41, 2240-2254, 10.1016/j.atmosenv.2006.03.049, 2007.

Shen, R., Schäfer, K., Schnelle-Kreis, J., Shao, L., Norra, S., Kramar, U., Michalke, B., Abbaszade, G., Streibel, T., Fricker, M., Chen, Y., Zimmermann, R., Emeis, S., and Schmid, H. P.: Characteristics and sources of PM in seasonal perspective – A case study from one year continuously sampling in Beijing, Atmospheric Pollution Research, 7, 235-248, 10.1016/j.apr.2015.09.008, 2016.

675   Song, H., Shang, J., Zhu, T., Zhao, L., and Ye, J. H.: Heterogeneous Oxidation of SO_2 by Ozone
676   on the Surface of Black Carbon Particles, Chem. J. Chin. Univ. Chin., 33, 2295-2302,
677   10.7503/cjcu20120024, 2012.

678   Sun, Y. L., Wang, Z. F., Fu, P. Q., Yang, T., Jiang, Q., Dong, H. B., Li, J., and Jia, J. J.: Aerosol
679   composition, sources and processes during wintertime in Beijing, China, Atmospheric Chemistry
680   and Physics, 13, 4577-4592, 10.5194/acp-13-4577-2013, 2013.

681   Tan, J., Duan, J., Zhen, N., He, K., and Hao, J.: Chemical characteristics and source of
682   size-fractionated atmospheric particle in haze episode in Beijing, Atmospheric Research, 167,
683   24-33, 10.1016/j.atmosres.2015.06.015, 2016.

684   Tang, G. Q., Chao, N., Wang, Y. S., and Chen, J. S.: Vehicular emissions in China in 2006 and
685   2010, Journal of Environmental Sciences, 48, 179-192, 10.1016/j.jes.2016.01.031, 2016.

686   Tao, M., Chen, L., Su, L., and Tao, J.: Satellite observation of regional haze pollution over the
687   North China Plain, Journal of Geophysical Research: Atmospheres, 117, 10.1029/2012jd017915,
688   2012.

689   Taylor, S. R.: Trace element abundances and the chondritic earth model, Geochimica Et
690   Cosmochimica Acta, 28, 1989-1998, 10.1016/0016-7037(64)90142-5, 1964.

691   Tian, S., Pan, Y., Liu, Z., Wen, T., and Wang, Y.: Size-resolved aerosol chemical analysis of
692   extreme haze pollution events during early 2013 in urban Beijing, China, J Hazard Mater, 279,
693   452-460, 10.1016/j.jhazmat.2014.07.023, 2014.

694   Underwood, G. M., Song, C. H., Phadnis, M., Carmichael, G. R., and Grassian, V. H.:
695   Heterogeneous reactions of NO_2 and HNO_3 on oxides and mineral dust: A combined laboratory
696   and modeling study, Journal of Geophysical Research: Atmospheres, 106, 18055-18066,
697   10.1029/2000jd900552, 2001.

698   Van Eyk, P. J., Ashman, P. J., and Nathan, G. J.: Mechanism and kinetics of sodium release from
699   brown coal char particles during combustion, Combustion and Flame, 158, 2512-2523,
700   10.1016/j.combustflame.2011.05.005, 2011.

701   Wang, G., Zhang, R., Gomez, M. E., Yang, L., Levy Zamora, M., Hu, M., Lin, Y., Peng, J., Guo,
702   S., Meng, J., Li, J., Cheng, C., Hu, T., Ren, Y., Wang, Y., Gao, J., Cao, J., An, Z., Zhou, W., Li, G.,
703   Wang, J., Tian, P., Marrero-Ortiz, W., Secrest, J., Du, Z., Zheng, J., Shang, D., Zeng, L., Shao, M.,
704   Wang, W., Huang, Y., Wang, Y., Zhu, Y., Li, Y., Hu, J., Pan, B., Cai, L., Cheng, Y., Ji, Y., Zhang, F.,
705   Rosenfeld, D., Liss, P. S., Duce, R. A., Kolb, C. E., and Molina, M. J.: Persistent sulfate formation
706   from London Fog to Chinese haze, Proceedings of the National Academy of Sciences of the
707   United States of America, 2016.

708   Wang, H., Zhou, Y., Zhuang, Y., Wang, X., and Hao, Z.: Characterization of $PM_{2.5}/PM_{2.5-10}$ and
709   source tracking in the juncture belt between urban and rural areas of Beijing, Chinese Science
710   Bulletin, 54, 2506-2515, 10.1007/s11434-009-0021-x, 2009.

711   Wang, H. L., Hao, Z. P., Zhuang, Y. H., Wang, W., and Liu, X. Y.: Characterization of inorganic
712   components of size-segregated particles in the flue gas of a coal-fired power plant, Energy &
713   Fuels, 22, 1636-1640, 10.1021/ef700527y, 2008.

714   Wang, Y., Zhuang, G. S., Tang, A. H., Yuan, H., Sun, Y. L., Chen, S. A., and Zheng, A. H.: The ion
715   chemistry and the source of $PM_{2.5}$ aerosol in Beijing, Atmospheric Environment, 39, 3771-3784,
716   10.1016/j.atmosenv.2005.03.013, 2005.

717   Wang, Y., Yao, L., Wang, L., Liu, Z., Ji, D., Tang, G., Zhang, J., Sun, Y., Hu, B., and Xin, J.:
718   Mechanism for the formation of the January 2013 heavy haze pollution episode over central and

eastern China, Science China Earth Sciences, 57, 14-25, 10.1007/s11430-013-4773-4, 2013.

Wen, W., Cheng, S., Chen, X., Wang, G., Li, S., Wang, X., and Liu, X.: Impact of emission control on $PM_{2.5}$ and the chemical composition change in Beijing-Tianjin-Hebei during the APEC summit 2014, Environmental science and pollution research international, 23, 4509-4521, 10.1007/s11356-015-5379-5, 2016.

Wu, L. Y., Tong, S. R., Wang, W. G., and Ge, M. F.: Effects of temperature on the heterogeneous oxidation of sulfur dioxide by ozone on calcium carbonate, Atmospheric Chemistry and Physics, 11, 6593-6605, 10.5194/acp-11-6593-2011, 2011.

Wu, S., Deng, F., Wei, H., Huang, J., Wang, X., Hao, Y., Zheng, C., Qin, Y., Lv, H., Shima, M., and Guo, X.: Association of cardiopulmonary health effects with source-appointed ambient fine particulate in Beijing, China: a combined analysis from the Healthy Volunteer Natural Relocation (HVNR) study, Environ Sci Technol, 48, 3438-3448, 10.1021/es404778w, 2014.

Xu, S. S., Liu, W. X., and Tao, S.: Emission of polycyclic aromatic hydrocarbons in China, Environ. Sci. Technol., 40, 702-708, 10.1021/es0517062, 2006.

Xu, W. Y., Zhao, C. S., Ran, L., Deng, Z. Z., Liu, P. F., Ma, N., Lin, W. L., Xu, X. B., Yan, P., He, X., Yu, J., Liang, W. D., and Chen, L. L.: Characteristics of pollutants and their correlation to meteorological conditions at a suburban site in the North China Plain, Atmospheric Chemistry and Physics, 11, 4353-4369, 10.5194/acp-11-4353-2011, 2011.

Yang, F., Tan, J., Zhao, Q., Du, Z., He, K., Ma, Y., Duan, F., Chen, G., and Zhao, Q.: Characteristics of $PM_{2.5}$ speciation in representative megacities and across China, Atmospheric Chemistry and Physics, 11, 5207-5219, 10.5194/acp-11-5207-2011, 2011.

Yang, X., Geng, C., Sun, X., Yang, W., Wang, X., and Chen, J.: Characteristics of particulate-bound polycyclic aromatic hydrocarbons emitted from industrial grade biomass boilers, J Environ Sci (China), 40, 28-34, 10.1016/j.jes.2015.09.010, 2016.

Yang, Y. R., Liu, X. G., Qu, Y., An, J. L., Jiang, R., Zhang, Y. H., Sun, Y. L., Wu, Z. J., Zhang, F., Xu, W. Q., and Ma, Q. X.: Characteristics and formation mechanism of continuous hazes in China: a case study during the autumn of 2014 in the North China Plain, Atmospheric Chemistry and Physics, 15, 8165-8178, 10.5194/acp-15-8165-2015, 2015.

Yao, L., Yang, L., Chen, J., Wang, X., Xue, L., Li, W., Sui, X., Wen, L., Chi, J., Zhu, Y., Zhang, J., Xu, C., Zhu, T., and Wang, W.: Characteristics of carbonaceous aerosols: Impact of biomass burning and secondary formation in summertime in a rural area of the North China Plain, The Science of the total environment, 557-558, 520-530, 10.1016/j.scitotenv.2016.03.111, 2016.

Yu, L. D., Wang, G. F., Zhang, R. J., Zhang, L. M., Song, Y., Wu, B. B., Li, X. F., An, K., and Chu, J. H.: Characterization and Source Apportionment of $PM_{2.5}$ in an Urban Environment in Beijing, Aerosol and Air Quality Research, 13, 574-583, 10.4209/aaqr.2012.07.0192, 2013.

Zhang, H., Wang, S., Hao, J., Wang, X., Wang, S., Chai, F., and Li, M.: Air pollution and control action in Beijing, Journal of Cleaner Production, 112, 1519-1527, 10.1016/j.jclepro.2015.04.092, 2016.

Zhang, Q., He, K. B., and Huo, H.: Cleaning China's air, Nature, 484, 161-162, 2012.

Zhang, R., Jing, J., Tao, J., Hsu, S. C., Wang, G., Cao, J., Lee, C. S. L., Zhu, L., Chen, Z., Zhao, Y., and Shen, Z.: Chemical characterization and source apportionment of $PM_{2.5}$ in Beijing: seasonal perspective, Atmospheric Chemistry and Physics, 13, 7053-7074, 10.5194/acp-13-7053-2013, 2013.

Zhang, R., Wang, G., Guo, S., Zamora, M. L., Ying, Q., Lin, Y., Wang, W., Hu, M., and Wang, Y.:

Formation of urban fine particulate matter, Chem Rev, 115, 3803-3855, 10.1021/acs.chemrev.5b00067, 2015.

Zhang, X. Y., Gong, S. L., Shen, Z. X., Mei, F. M., Xi, X. X., Liu, L. C., Zhou, Z. J., Wang, D., Wang, Y. Q., and Cheng, Y.: Characterization of soil dust aerosol in China and its transport and distribution during 2001 ACE-Asia: 1. Network observations, Journal of Geophysical Research: Atmospheres, 108, 10.1029/2002jd002632, 2003.

Zhang, Y., Schauer, J. J., Zhang, Y., Zeng, L., Wei, Y., Liu, Y., and Shao, M.: Characteristics of particulate carbon emissions from real-world Chinese coal combustion, Environ. Sci. Technol., 42, 5068-5073, 10.1021/es7022576, 2008.

Zhang, Z., Wang, H., Chen, D., Li, Q., Thai, P., Gong, D., Li, Y., Zhang, C., Gu, Y., Zhou, L., Morawska, L., and Wang, B.: Emission characteristics of volatile organic compounds and their secondary organic aerosol formation potentials from a petroleum refinery in Pearl River Delta, China, The Science of the total environment, 584-585, 1162-1174, 10.1016/j.scitotenv.2017.01.179, 2017.

Zhao, P. S., Dong, F., He, D., Zhao, X. J., Zhang, X. L., Zhang, W. Z., Yao, Q., and Liu, H. Y.: Characteristics of concentrations and chemical compositions for $PM_{2.5}$ in the region of Beijing, Tianjin, and Hebei, China, Atmospheric Chemistry and Physics, 13, 4631-4644, 10.5194/acp-13-4631-2013, 2013a.

Zhao, P. S., Dong, F., Yang, Y. D., He, D., Zhao, X. J., Zhang, W. Z., Yao, Q., and Liu, H. Y.: Characteristics of carbonaceous aerosol in the region of Beijing, Tianjin, and Hebei, China, Atmospheric Environment, 71, 389-398, 10.1016/j.atmosenv.2013.02.010, 2013b.

Zhao, X. J., Zhao, P. S., Xu, J., Meng, W., Pu, W. W., Dong, F., He, D., and Shi, Q. F.: Analysis of a winter regional haze event and its formation mechanism in the North China Plain, Atmospheric Chemistry and Physics, 13, 5685-5696, 10.5194/acp-13-5685-2013, 2013.

Zhao, Y., Ma, Q., Liu, Y., and He, H.: Influence of sulfur in fuel on the properties of diffusion flame soot, Atmospheric Environment, 142, 383-392, 10.1016/j.atmosenv.2016.08.001, 2016.

Zheng, B., Zhang, Q., Zhang, Y., He, K. B., Wang, K., Zheng, G. J., Duan, F. K., Ma, Y. L., and Kimoto, T.: Heterogeneous chemistry: a mechanism missing in current models to explain secondary inorganic aerosol formation during the January 2013 haze episode in North China, Atmospheric Chemistry and Physics, 15, 2031-2049, 10.5194/acp-15-2031-2015, 2015.

Zheng, G. J., Duan, F. K., Su, H., Ma, Y. L., Cheng, Y., Zheng, B., Zhang, Q., Huang, T., Kimoto, T., Chang, D., Pöschl, U., Cheng, Y. F., and He, K. B.: Exploring the severe winter haze in Beijing: the impact of synoptic weather, regional transport and heterogeneous reactions, Atmospheric Chemistry and Physics, 15, 2969-2983, 10.5194/acp-15-2969-2015, 2015.

Zong, Z., Wang, X., Tian, C., Chen, Y., Qu, L., Ji, L., Zhi, G., Li, J., and Zhang, G.: Source apportionment of $PM_{2.5}$ at a regional background site in North China using PMF linked with radiocarbon analysis: insight into the contribution of biomass burning, Atmospheric Chemistry and Physics, 16, 11249-11265, 10.5194/acp-16-11249-2016, 2016.
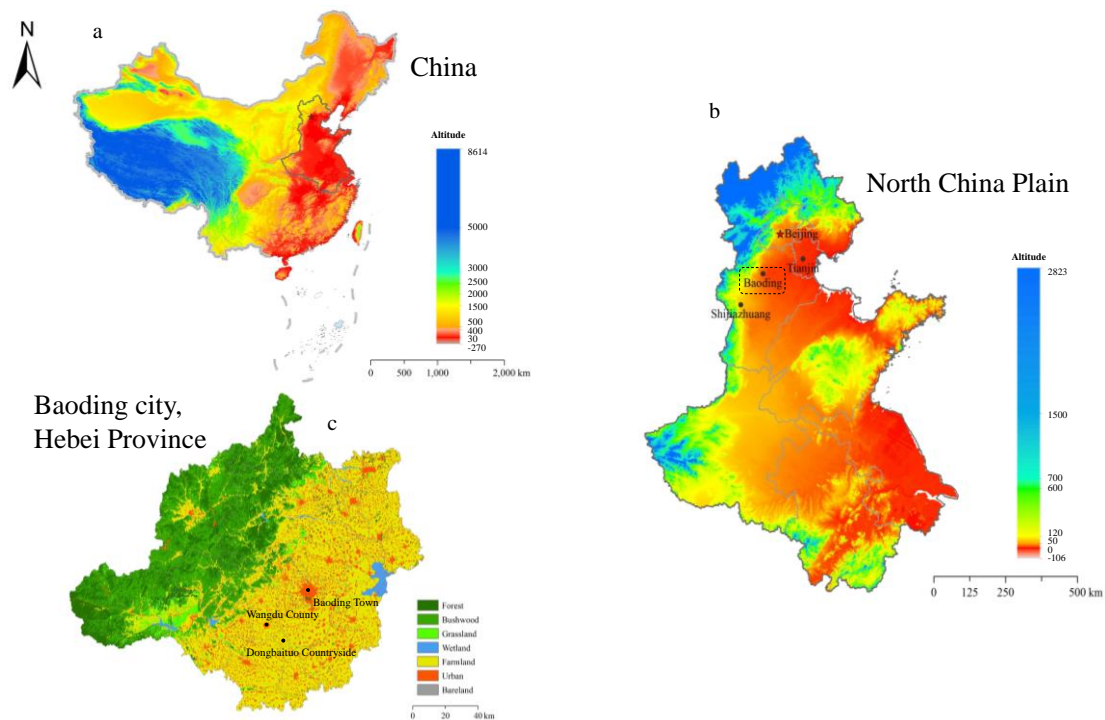
803

804   **Figure 1.** China (a), the North China Plain (b) and Baoding city in Hebei Province (c). The
805   locations of sampling sites (BJ, BD, WD and DBT) as well as Tianjin municipality and
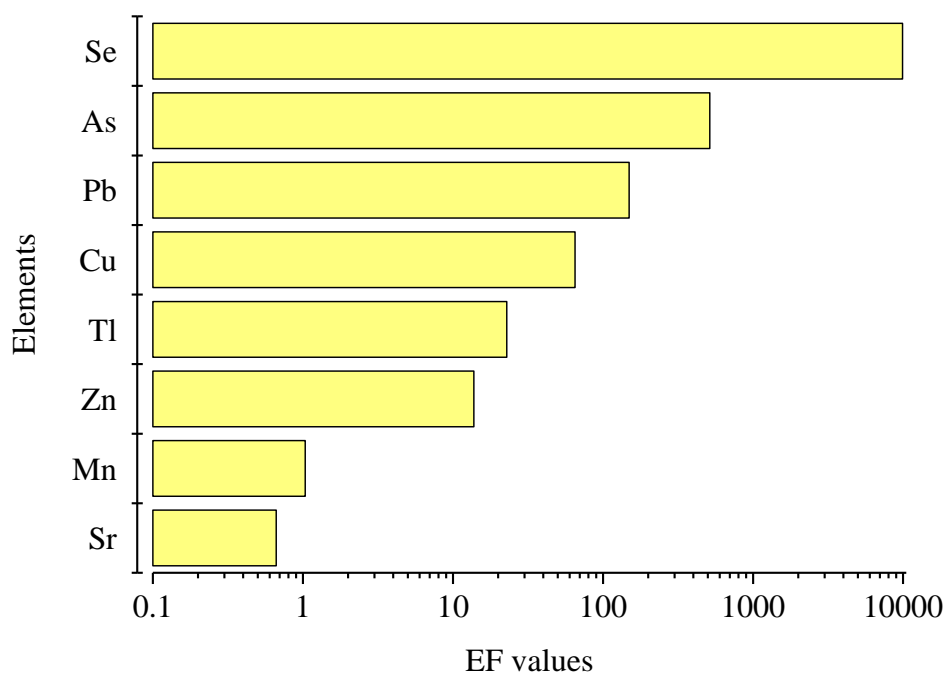806   Shijiazhuang as provincial capital of Hebei are marked.

807

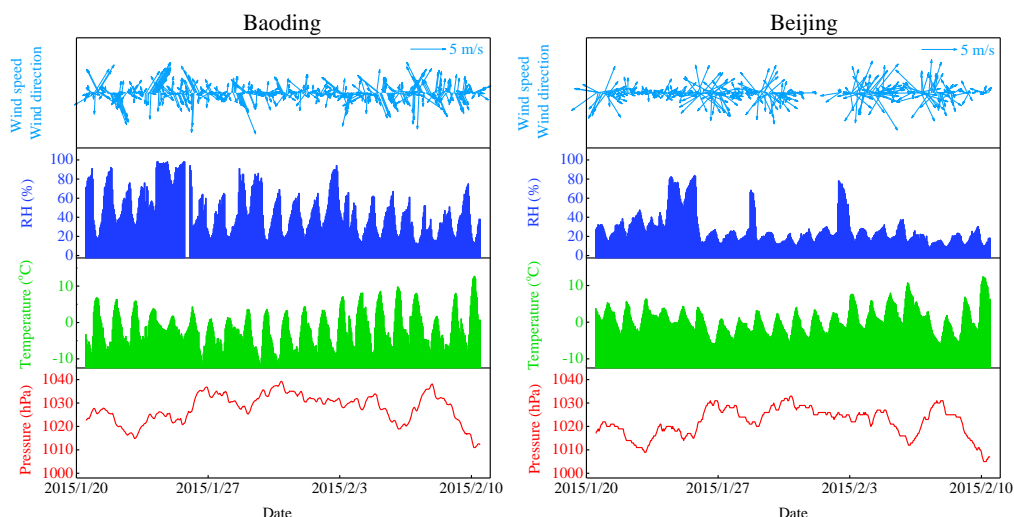808   **Figure 2.** Enrichment factor values for trace elements in PM$_{2.5}$.

29

809

Figure 3. The wind speed, wind direction, RH, temperature and barometric pressure at BD and BJ during the sampling period in the winter of 2015.
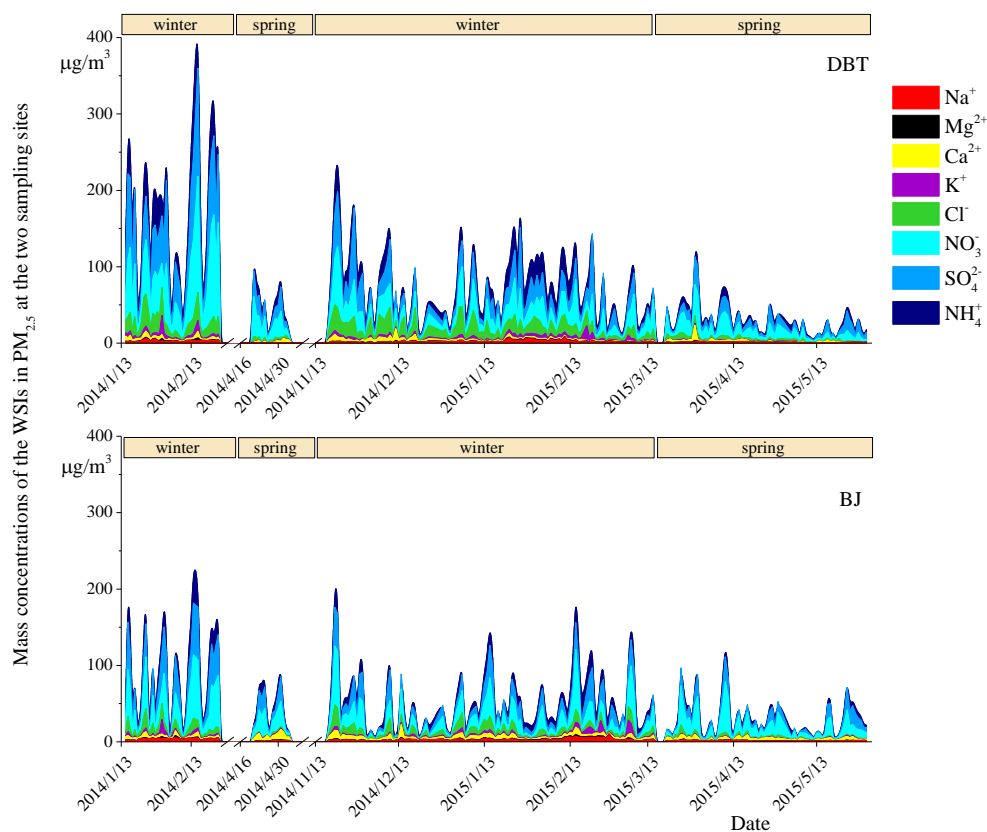

812

Figure 4. The mass concentrations of the WSIs in PM$_{2.5}$ at DBT and BJ during the sampling period in the winters and springs of 2014-2015.
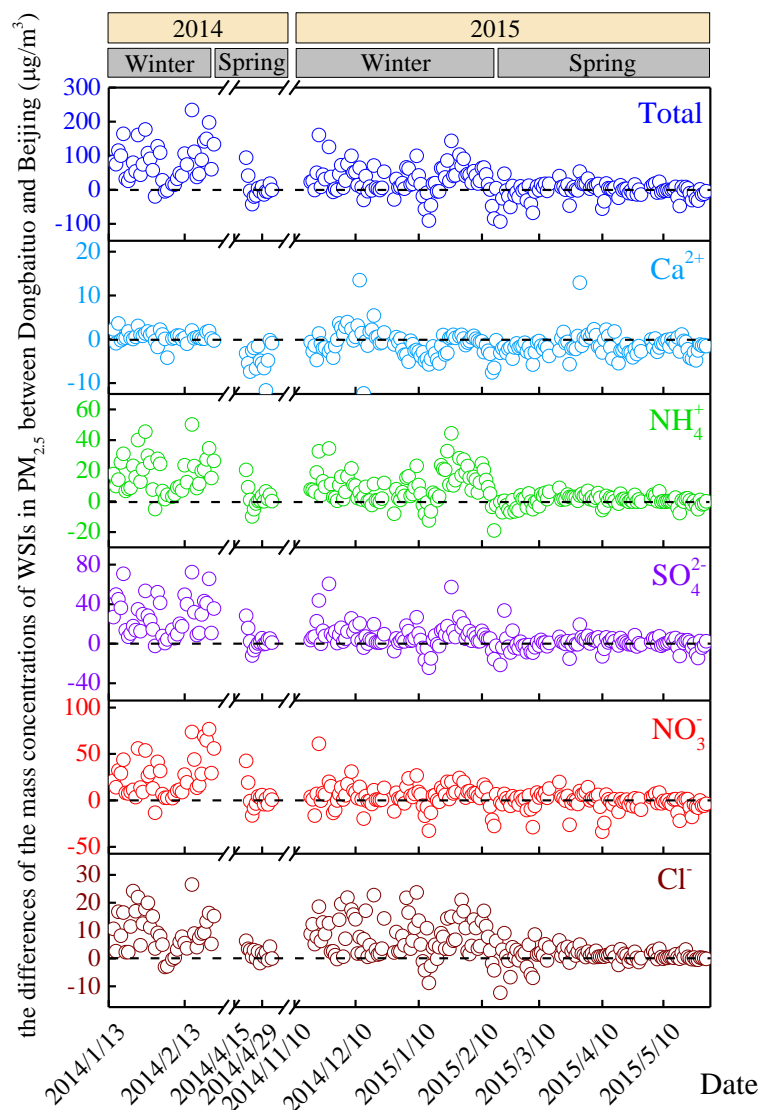
Figure 5. The D-values of the mass concentrations of WSIs in PM$_{2.5}$ between DBT and BJ during the sampling period in the winters and springs of 2014-2015.
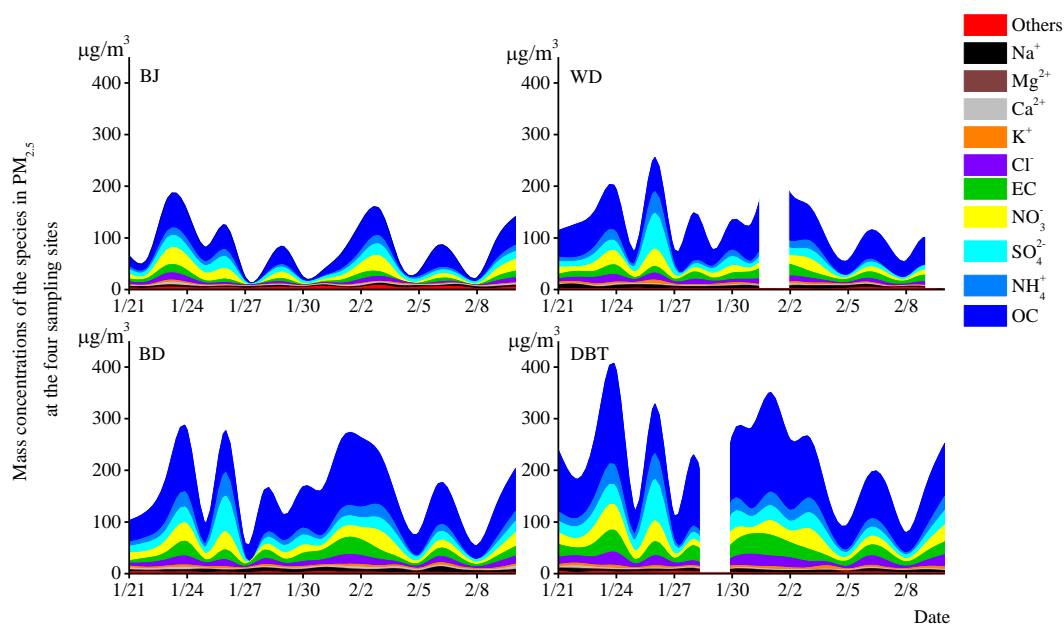
818

819 **Figure 6.** Daily variation of the species in PM₂.₅ at the four sampling sites during the sampling
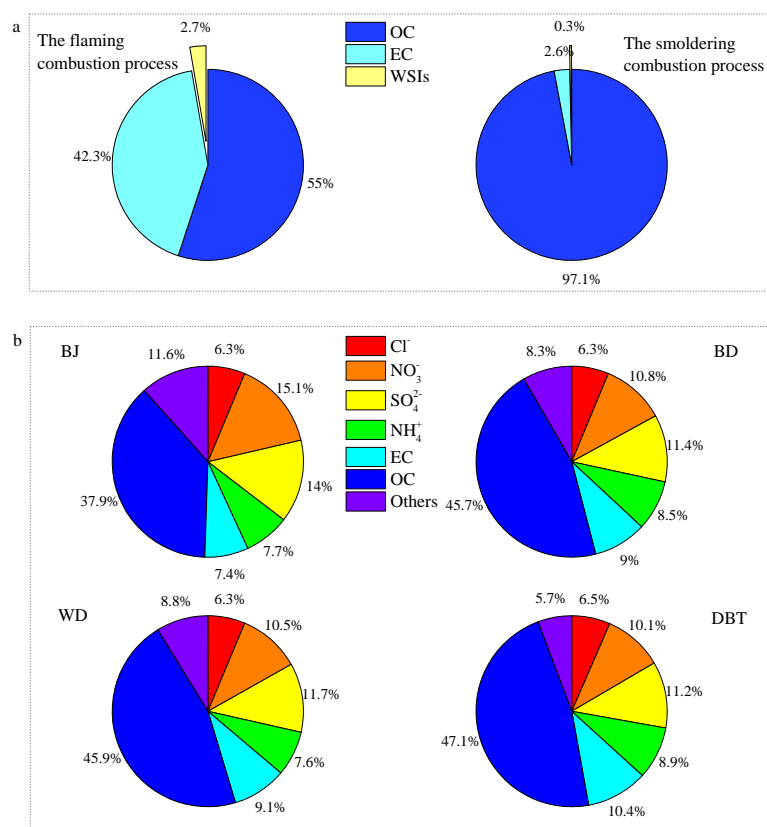820 period in the winter of 2015.

821

822 **Figure 7.** The mass proportions of OC, EC and WSIs from residential coal combustion under the
823 flaming and smoldering combustion processes (a), and the average mass proportions of the typical

824   species in PM$_{2.5}$ at the four sampling sites during the sampling period in the winter of 2015 (b).

Backward trajectories
Cluster means – Standard
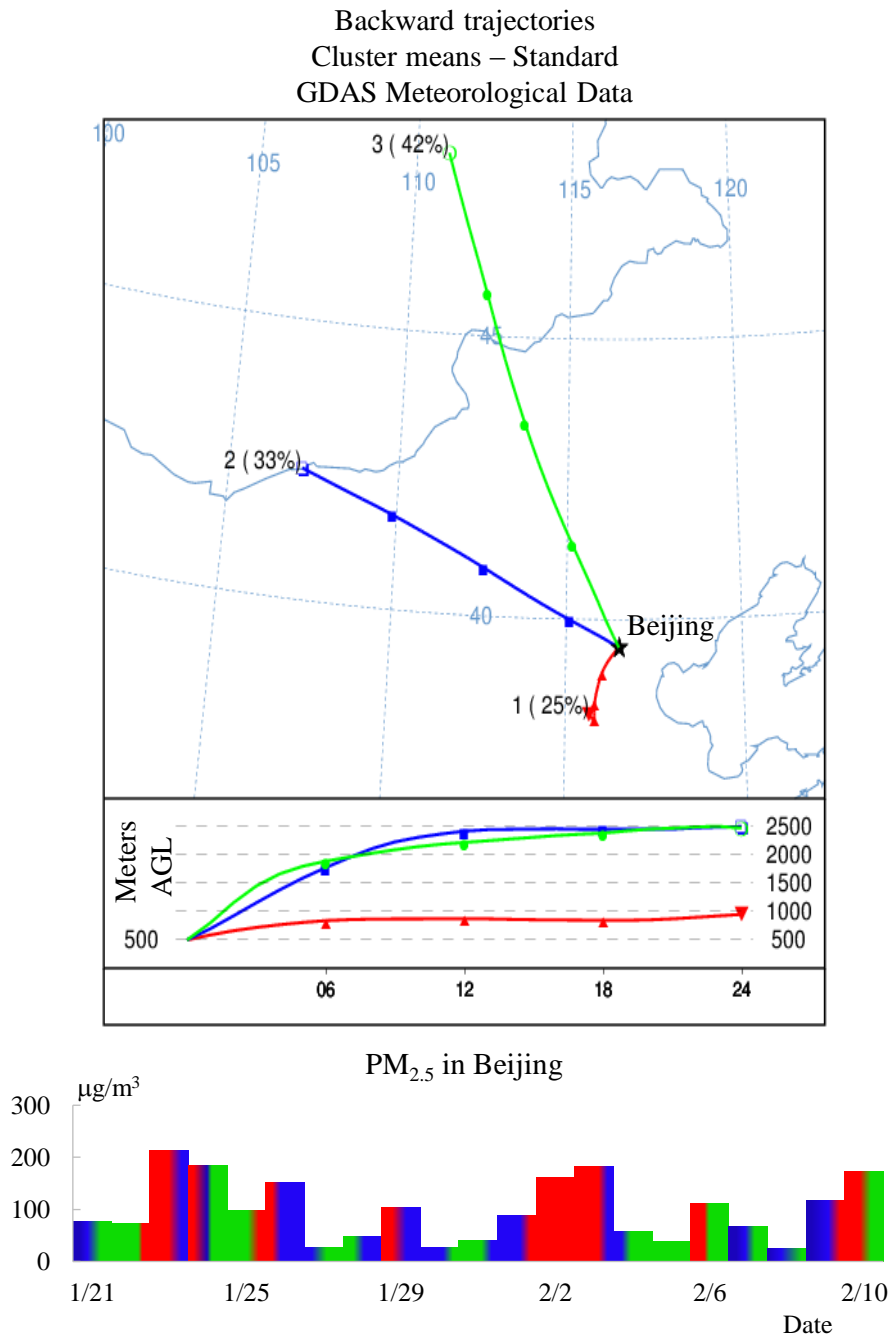GDAS Meteorological Data

825

826   **Figure 8.** The back trajectory cluster analysis and the corresponding PM$_{2.5}$ concentrations in

827   Beijing during the sampling period in the winter of 2015.
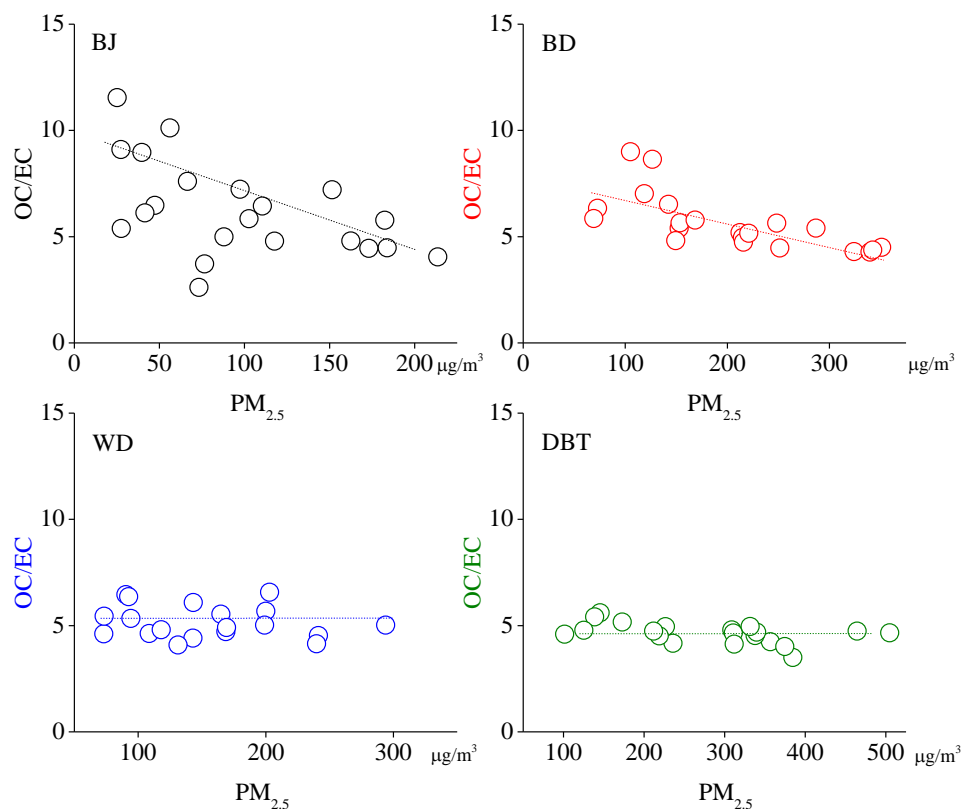
828

829

Figure 9. The correlations between the OC/EC ratios and the PM$_{2.5}$ concentrations at the four sampling sites during the sampling period in the winter of 2015.

832
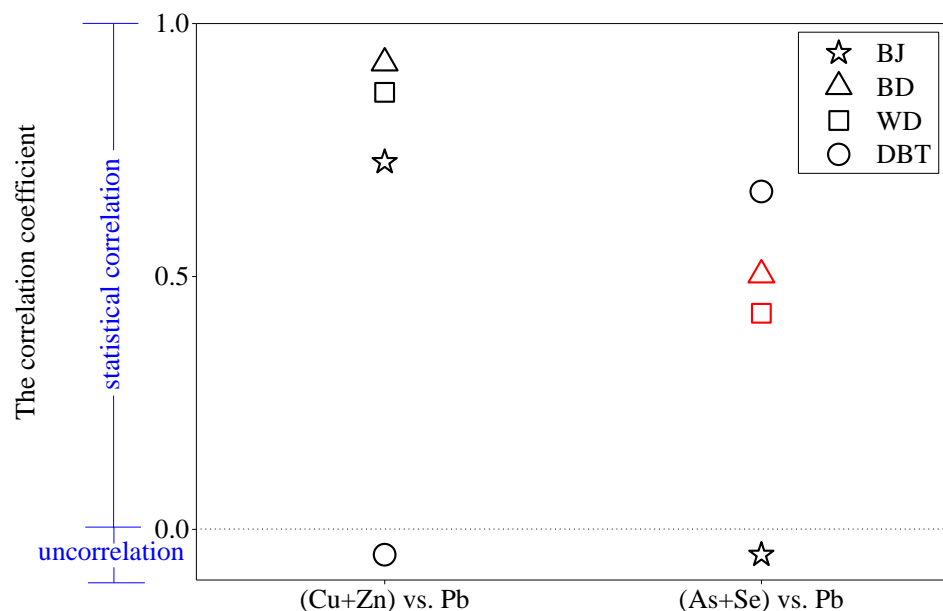
Figure 10. The statistical correlations for [Cu+Zn] vs. [Pb] and [As+Se] vs. [Pb] in PM$_{2.5}$ at the four sampling sites during the sampling period in the winter of 2015. The uncorrelated results are

also marked below zero of Y axis. The red and black symbols represent for $p < 0.05$ and $p < 0.01$, respectively.

Figure 11. The proportions of source species under the constructed chemical mass closures for PM$_{2.5}$ at the four sampling sites during the sampling period in the winter of 2015. Average mass concentrations of PM$_{2.5}$ at each sampling site, including all of source species and unidentified fractions, are also marked at the top of bar charts.

843 **Figure 12.** The estimated contributions of coal combustion to the PM$_{2.5}$ at the four sampling sites
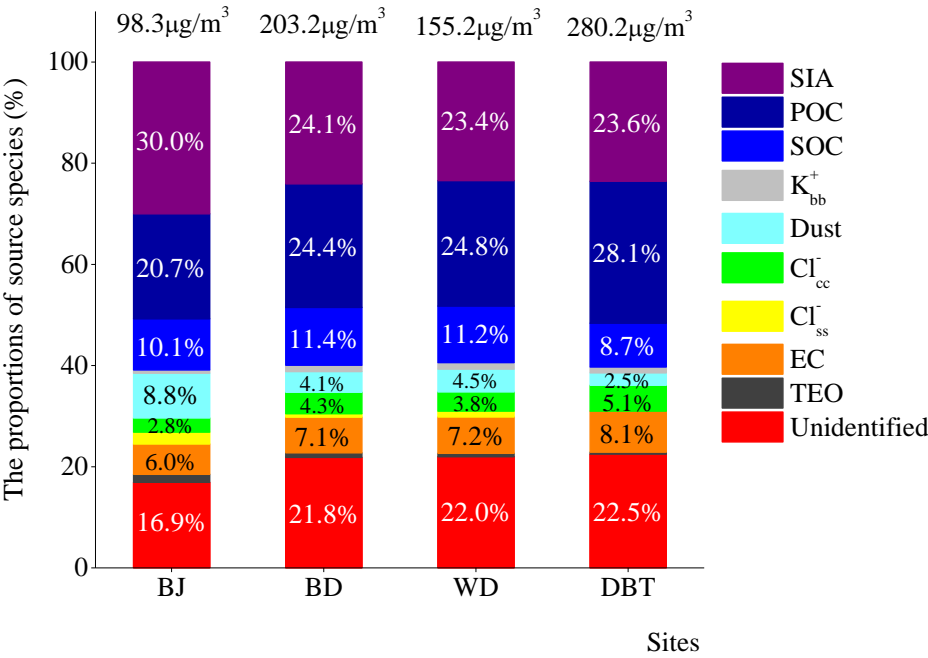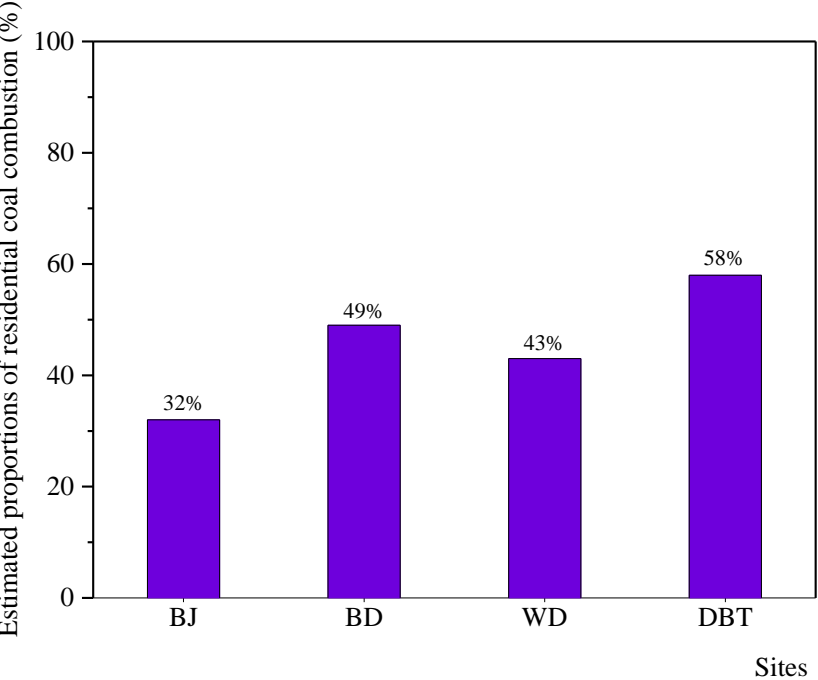844 during the sampling period in the winter of 2015.

845

846 **Table 1.** The average mass concentrations of WSIs in PM$_{2.5}$ at DBT and BJ during the sampling
847 period in the winters and springs of 2014-2015 (μg m^{-3}).

WSIs	spring		winter	
	DBT	BJ	DBT	BJ
Na$^+$	1.0 ±0.5	1.4 ±0.5	2.4 ±1.3	3.1 ±1.4
Mg^{2+}	0.2 ±0.2	0.3 ±0.2	0.7 ±0.5	0.8 ±0.7
Ca^{2+}	1.7 ±2.4	3.4 ±2.5	2.6 ±2.1	3.4 ±2.3
K$^+$	0.5 ±0.5	0.7 ±0.4	3.2 ±3.0	3.0 ±6.0
NH$_4^+$	6.1 ±5.1	4.8 ±4.7	23.1 ±17.9	13.2 ±11.6
NO$_3^-$	12.5 ±11.2	13.6 ±13.2	28.4 ±28.0	19.0 ±20.0
SO$_4^{2-}$	10.5 ±8.2	9.2 ±8.6	29.0 ±28.1	17.4 ±16.5
Cl$^-$	2.9 ±2.2	1.8 ±1.6	14.1 ±9.4	7.2 ±6.0
Total	35.3 ±26.7	35.1 ±28.7	103.3 ±81.3	67.0 ±55.2

848

849 **Table 2.** The average mass concentrations (Mean ±SD) of PM$_{2.5}$ species, NO$_2$ and SO$_2$ at the four
850 sampling sites during the sampling period in the winter of 2015 (μg m^{-3}).

Species	BJ	BD	WD	DBT
Na$^+$	2.5 ±0.7	4.8 ±2.0	4.5 ±1.7	4.3 ±1.2
Mg^{2+}	0.3 ±0.1	0.4 ±0.1	0.3 ±0.1	0.4 ±0.2
Ca^{2+}	1.8 ±0.9	2.6 ±0.8	1.7 ±0.6	2.0 ±0.8
K$^+$	0.7 ±0.8	2.5 ±1.0	2.0 ±1.4	3.1 ±1.3
NH$_4^+$	6.0 ±5.0	13.3 ±11.0	9.3 ±9.5	18.7 ±11.7
NO$_3^-$	11.7 ±10.1	16.6 ±10.3	13.0 ±8.2	21.0 ±12.2
SO$_4^{2-}$	11.2 ±6.5	18.1 ±14.1	14.5 ±14.5	24.1 ±16.1
Cl$^-$	5.0 ±3.6	9.5 ±4.2	7.8 ±3.5	13.4 ±6.0
OC	28.6 ±19.6	70.2 ±31.2	57.2 ±21.3	100.0 ±42.9
EC	5.5 ±4.5	13.5 ±7.8	11.4 ±4.7	21.6 ±10.2
Al	0.6 ±0.8	0.6 ±0.1	0.5 ±0.2	0.5 ±0.1
Mn	0.1 ±0.1	0.1 ±0.1	0.1 ±0.1	0.2 ±0.3
Fe	2.1 ±0.8	0.6 ±0.2	0.8 ±0.6	1.3 ±0.6
Cu	0.6 ±0.3	0.3 ±0.1	0.2 ±0.1	0.1 ±0.1
Zn	0.1 ±0.1	0.2 ±0.1	0.1 ±0.1	0.1 ±0.1
As	0.1 ±0.1	0.3 ±0.1	0.2 ±0.1	0.1 ±0.1
Se	0.1 ±0.0	0.1 ±0.1	0.1 ±0.0	0.1 ±0.0
Sr	0.0 ±0.0	0.1 ±0.0	0.0 ±0.0	0.0 ±0.0
Tl	0.0 ±0.0	0.0 ±0.0	0.0 ±0.0	0.0 ±0.0
Pb	0.2 ±0.2	0.4 ±0.3	0.2 ±0.1	0.3 ±0.1
The total	80.1 ±47.7	159.5 ±70.3	121.7 ±51.8	218.4 ±87.1
NO$_2$	36.5 ±17.4	60.4 ±23.4	76.1 ±19.2	-
SO$_2$	63.9 ±31.7	181.7 ±62.4	101.3 ±39.4	-

851

852 **Table 3.** The emission factors (Mean $\pm$ SD) (g kg^{-1} coal) of OC and EC from residential coal
853 combustion during the flaming combustion process, the smoldering combustion process and the
854 entire combustion process.

Emission factors	the flaming combustion process	the smoldering combustion process	the entire combustion process
OC	1.83 $\pm$ 1.19	17.11 $\pm$ 0.79	10.99 $\pm$ 0.95
EC	1.40 $\pm$ 0.11	0.46 $\pm$ 0.03	0.84 $\pm$ 0.06

855

856 **Table 4.** The correlations of several typical species in PM$_{2.5}$ at the four sampling sites during the
857 sampling period in the winter of 2015.

n=21 BJ	Mg^{2+}	Ca^{2+}	K^+	Cl^-	NO_3^-	SO_4^{2-}	NH_4^+	OC	EC
Mg^{2+}	1								
Ca^{2+}	0.895**	1							
K^+	0.634**	0.862**	1						
Cl^-	0.856**	0.899**	0.791**	1					
NO_3^-	0.803**	0.768**	0.637**	0.905**	1				
SO_4^{2-}	0.679**	0.660**	0.590**	0.804**	0.950**	1			
NH_4^+	0.718**	0.667**	0.543*	0.834**	0.971**	0.959**	1		
OC	0.845**	0.751**	0.560**	0.848**	0.919**	0.838**	0.895**	1	
EC	0.849**	0.851**	0.679**	0.932**	0.877**	0.769**	0.823**	0.936**	1

n=21 BD	Mg^{2+}	Ca^{2+}	K^+	Cl^-	NO_3^-	SO_4^{2-}	NH_4^+	OC	EC
Mg^{2+}	1								
Ca^{2+}	0.805**	1							
K^+	0.697**	0.556**	1						
Cl^-	0.714**	0.659**	0.789**	1					
NO_3^-	0.554**	0.560**	0.675**	0.757**	1				
SO_4^{2-}	0.022	0.107	0.491*	0.499*	0.764**	1			
NH_4^+	0.315	0.331	0.659**	0.721**	0.920**	0.941**	1		
OC	0.743**	0.576**	0.705**	0.936**	0.674**	0.369	0.614**	1	
EC	0.698**	0.560**	0.702**	0.939**	0.660**	0.410	0.633**	0.984**	1

n=19 WD	Mg^{2+}	Ca^{2+}	K^+	Cl^-	NO_3^-	SO_4^{2-}	NH_4^+	OC	EC
Mg^{2+}	1								
Ca^{2+}	0.897**	1							
K^+	0.226	0.457*	1						
Cl^-	0.532*	0.663**	0.598**	1					
NO_3^-	0.468*	0.677**	0.712**	0.796**	1				
SO_4^{2-}	0.097	0.358	0.874**	0.552*	0.770**	1			
NH_4^+	0.306	0.563**	0.906**	0.735**	0.901**	0.945**	1		
OC	0.463*	0.543*	0.372	0.816**	0.471*	0.222	0.581*	1	
EC	0.553*	0.638**	0.339	0.763**	0.510*	0.214	0.565*	0.925**	1

n=20	DBT								
	Mg^{2+}	Ca^{2+}	K^+	Cl^-	NO_3^-	SO_4^{2-}	NH_4^+	OC	EC
Mg^{2+}	1								
Ca^{2+}	0.721**	1							
K^+	0.191	0.407	1						
Cl^-	-0.061	0.316	0.519*	1					
NO_3^-	-0.241	0.161	0.579**	0.642**	1				
SO_4^{2-}	-0.133	0.109	0.458*	0.482*	0.744**	1			
NH_4^+	-0.223	0.125	0.558*	0.697**	0.928**	0.914**	1		
OC	0.067	0.159	0.419	0.772**	0.570**	0.293	0.557*	1	
EC	0.051	0.169	0.419	0.838**	0.585**	0.400	0.624**	0.977**	1

858   *, ** represent for $p < 0.05$ and $p < 0.01$, respectively.

859

860   **Table 5.** The correlations between [Zn] vs. [Cu] and [As] vs. [Se] in $PM_{2.5}$ at the four sampling
861   sites during the sampling period in the winter of 2015.

Elements	BJ (n=21)	BD (n=21)	WD (n=19)	DBT (n=20)
[Zn] vs. [Cu]	0.607**	0.479*	0.620*	0.659**
[As] vs. [Se]	0.662**	0.664**	0.959**	0.871**

862   *, ** represent for $p < 0.05$ and $p < 0.01$, respectively.

863
864
865
866
867
868
869
870
871
872
873
874
875
876
877
878
879
880
881
882